THE USE OF FLUORESCENCE TO INVESTIGATE THE FACTORS LEADING TO COMPLEX FORMATION BETWEEN NAPHTHALENES AND β-CYCLODEXTRINS

THE USE OF CAPILLARY ELECTROPHORESIS WITH CYCLODEXTRIN ADDITIVES FOR THE SEPARATION OF LSD, LAMPA, AND iso-LSD

By

Jamie M. Iannacone

****

Submitted in partial fulfillment
of the requirements for
Honors in the Department of Chemistry

UNION COLLEGE
June, 2003

ABSTRACT

IANNACONE, JAMIE M. The use of fluorescence to investigate the factors leading to complex formation between naphthalenes and β-cyclodextrins. Department of Chemistry, June 2003.

Fraiji et. al. determined a binding constant (K) of 581 ± 6 M^{-1} for the 1:1 complex between 2-acetylnaphthalene (2-AN) and β-cyclodextrin (β-CD) in H_2O using fluorescence quenching experiments (*Appl. Spectrosc.* 1994, 48, 79). Molecular modeling experiments indicate the possibility of complex stabilization resulting from hydrogen bonds between the C=O group of 2-AN and the -OH groups on the rim of β-CD. To check this possibility, we measured the K of the 2-AN:trimethyl-β-CD (TM-β-CD) complex, where all rim -OH groups are converted to $-OCH_3$. In this case, K decreases to 134 M^{-1}. To show that this is due to reduced hydrogen bonding capability rather than steric influence, the K of 2-AN:β-CD was measured at high pH. K decreases to 276 M^{-1} at pH 13.5, and an inflection point is observed at pH 12.2 (which is the pKa of rim -OH groups). Therefore, our experiments confirm the significance of 2-AN carbonyl hydrogen bonding to β-CD -OH groups.

Fluorescence studies were also performed with 1,5-DNSA, 2,6-MANS, and 2,6-TNS. K was 151 M^{-1} for 1,5-DNSA:β-CD and 105 M^{-1} for 1,5-DNSA:TM-β-CD. The smaller K for the TM-β-CD complex is probably due to steric effects associated with the rim $-OCH_3$ groups. Thermodynamic properties of the 2,6-MANS:TM-β-CD complex were investigated. ΔH and ΔS were calculated as –35 kJ/mol and –47 J/mol K, respectively. Catena and Bright calculated ΔH as –6.7 kJ/mol and ΔS as 50 J/mol K for the 2,6-MANS:β-CD complex (*Anal. Chem.* 1989, 61, 915). The methyl groups of the TM-β-CD make the cavity environment more hydrophobic than the natural β-CD, creating much stronger guest:host interations. The methyl groups also restrict the motion of 2,6-MANS, which overcomes the favored entropic effects of solvent replacement and solvent shell disturbance. The 2,6-TNS:TM-β-CD, K was calculated as 2358 M^{-1}, compared to Catena and Bright's 1980 M^{-1} for the β-CD complex. The more hydrophobic cavity of TM-β-CD compensates for the loss of hydrogen bonding between the guest SO_3^- group and CD rim –OH groups.

ABSTRACT

IANNACONE, JAMIE M. The use of capillary electrophoresis with cyclodextrin additives for the separation of LSD, LAMPA, and iso-LSD. Department of Chemistry, June 2003.

CE was employed for the separation of LSD (D-lysergic acid diethylamide), LAMPA (D-lysergic acid methylpropylamide) and iso-LSD using several types of cyclodextrins as buffer additives. A sample consisting of LSD, LAMPA, and iso-LSD was partially resolved (R>1) with 60 mM α-CD in a 50 mM acetate buffer, pH 4.03, at 15 °C. Migration times were under 9 min. Another solution consisting of both 60 mM α-CD and 0.2 mM sulfated-β-CD in 50 mM acetate buffer, pH 4.03, at 25 °C provided baseline separation (R>1.5) of the sample mixture in a similar 9 min. time window. The reproducibility of migration times for both methods was 4-5% between days and 1% on the same day. Partial separation of LSD and LAMPA (R ~1) was observed in a 9 min. time window using 15 mM sulfated-α-CD in a 50 mM borate buffer, pH 8.51 at 25 °C. Between day and same day reproducibilities were 2-3% and 1%, respectively.

ACKNOWLEDGEMENTS

This work is dedicated to the stellar Chemistry Department of Union College. I admire and graciously thank every one of its members.

Professor Werner, I would like to thank you for your expert guidance throughout my academic career. My research experience and graduate school decision would not have been the same without you. Thank you for challenging, encouraging, and believing in me as a person, and as a chemist.

Professor Carroll, thank you for exposing me to the world of chemistry, both academically and professionally. You have certainly made an impressive place for yourself and I only hope I can do the same.

Professors Hagerman, Kehlbeck, and Schnabel, thank you for teaching me how a chemist can have intellect, style, *and* a good time.

Kathy Ryan, you are hard working, dedicated, and truly wonderful. Thank you for letting me get to know you and for four years of laughter and chaos.

Desirée Plata and Bob Herbst, you have both been there for me from the very beginning. The past four years certainly wouldn't have been the same without you. Good luck and may all your dreams come true.

I would also like to acknowledge my family and friends for their support and encouragement. I owe a special thanks to my sister, Jodie, for teaching me chemistry.

TABLE OF CONTENTS

TABLE OF FIGURES

Part I.

Part II.

TABLE OF TABLES

Part I.

Part II.

Part I.
The Use of Fluorescence to Investigate the Factors Leading to Complex Formation Between Naphthalenes and β-Cyclodextrins.

INTRODUCTION

Cyclodextrins (CDs) are interesting molecules with many potential applications. α-, β-, and γ-cyclodextrins are composed of six, seven, or eight glucopyranose units, respectively, joined by α-(1,4)-linkages. Cyclodextrins are torroidal in shape and possess a hydrophobic inner cavity ranging from 0.57 – 0.95 nm in diameter,[1a] Figure 1.[1b] The non-polar environment of the cavity is ideal for attracting organic molecules from a more polar solvent. The inclusion complex that results is referred to as a host:guest interaction and is involved with applications in a variety of scientific fields.

Cyclodextrin inclusion complexes have been beneficial in analytical, industrial, and pharmaceutical science. They enhance the solubility of organic molecules in polar solvents, and are also important in separation science. Investigators have used CDs to differentiate between similarly structured molecules and isomers, including enantiomeric forms of chiral molecules. They have been used as modifiers in HPLC mobile phases, and can also improve detection limits by enhancing the fluorescent properties of licit and illicit drugs.[2,3] CDs have the ability to control dye aggregation equilibria, and can lead to a better understanding of protein-enzyme complexes.[4,5] Industrially, cyclodextrins are used to preserve the fragrant properties of soaps and detergents. CDs have also shown potential as drug delivery agents in pharmaceuticals.[6]

Figure 1. Structure of the natural cyclodextrin.

a. side view b. top view

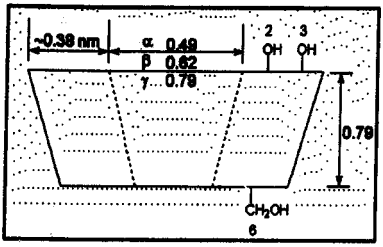
~0.38 nm
α 0.49
β 0.62
γ 0.79
2
3
OH
OH
0.79
CH2OH
6

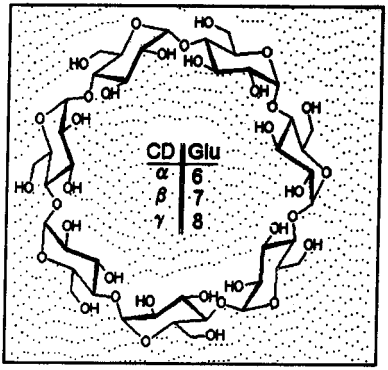
CD | Glu
α | 6
β | 7
γ | 8

While no one effect completely controls the extent of complex formation with cyclodextrins, it is understood that a variety of effects can each have an influence. Most importantly, the structures of both the CD host and the organic guest govern the binding characteristics. The CD cavity, as well as the type of substituents on the rim, determines how well the guest binds to a given CD. The hydroxyl groups on the unsubstituted CD rim, for example, provide the opportunity of forming hydrogen bonds with guest molecules. The methyl groups on the trimethyl-β-CD (TM-β-CD) rim, however, are bulky and may prevent the complete inclusion of the guest molecule. The groups also produce an extended, more hydrophobic cavity. Furthermore, the methylation of the hydroxyl groups eliminates the opportunity of forming hydrogen bonds at the rim. The size, as well as the functional groups of the guest, can also affect the binding interactions with a cyclodextrin.

The CD:guest formation reaction can be characterized thermodynamically. The reaction occurs with a change in enthalpy, as well as a change in entropy. The enthalpy change for most CD inclusion reactions is negative due to the hydrophobic interactions with the CD walls.[4] The entropy of the system, however, is a balance of factors and can be positive or negative. Through the hydrophobic effect, entropy is gained as the guest molecule enters the non-polar cavity, replacing the polar water molecules, and disrupting the low entropy solvent shell surrounding the guest. By contrast, a loss in entropy is observed as the guest is constrained in the cavity. The entropy change of a CD inclusion complex formation reaction is favorable when a large and positive value is calculated.

Fluorescence studies can be used to determine a binding constant specific for a certain guest:host interaction at a given temperature. Upon complexation, the

fluorescence intensity of organic probe molecules is often enhanced. This fluorescence enhancement is attributed to a series of factors, including the protection of the guest molecule from external quenchers, the absence of the free rotor effect upon complexation, and the less polar environment inside the CD cavity.[7] In some cases, however, complex formation is characterized by a decrease in fluorescent signal, or quenching. When the quenching is due to a complex in its ground state, the quenching is referred to as static.[8]

Fraiji et. al. investigated the binding characteristics of 2-acetylnaphthalene (2-AN) with β-CD using fluorescence quenching experiments. A binding constant of 581 ± 6 M^{-1} was determined for the entropically favored reaction.[8] Later, Madrid and Mendicuti used fluorescence spectral shifts to determine the binding constant for the 2-methylnaphthoate (2-MN):β-CD system as 1965 ± 159 M^{-1}; this is more than three times the value determined for the 2-acetylnapthalene complex.[9] The significant difference, according to Madrid and Mendicuti, was due to the increased stabilization of the complex by hydrogen bonds between the ester oxygen atom of 2-MN and the hydroxyl groups on the CD rim. Werner et. al., however, came to a different conclusion upon performing molecular modeling studies along with fluorescence experimentation.[10] Werner and co-workers modeled the inclusion complex of 2-MN with β-CD, along with similar complexes involving several derivatives of 2-naphthylamide. These derivatives also provided the opportunity of stabilization by hydrogen bonds with the amide nitrogen, as well as with the hydrogen atoms on the amide. Molecular modeling studies, however, showed that both the 2-MN ester oxygen and the amide nitrogen are sticking out the middle of the cavity, and not close enough for hydrogen bonding with the CD rim.

Furthermore, the experimental work resulted in binding constants for the amide naphthalene derivatives on the order of 500-600 M^{-1}, about a third of the K value determined for 2-MN. Werner et. al. contribute the significant differences in K values to the different polarities of the guest molecules. The dipole moment of the 2-MN molecule is significantly lower than the dipole moment of the other naphthalene derivatives. Thus, 2-MN would be attracted to the hydrophobic interior of the CD cavity more strongly than the other guests.[10]

One goal of this experiment is to use fluorescence quenching experiments to show whether the oxygen from the carbonyl group of the 2-AN guest can hydrogen bond with the hydroxyl groups on the β-CD rim. There is modeling evidence to indicate that this could occur.[10] And, if so, is this hydrogen bonding interaction a significant factor in complex formation?

We investigated the complexation of 2-AN with TM-β-CD and with β-CD at high pH. TM-β-CD has no rim hydroxyl groups, and hydrogen bonding between the carbonyl oxygen of the guest and the CD rim is thereby prohibited. In addition, the formation of the inclusion complex may be sterically hindered by the methyl groups on the CD rim. Also, in an environment of high pH, the hydroxyl groups on the β-CD rim are deprotonated and lose their ability to hydrogen bond. The binding constants of the different host:guest complexes, when compared to the results of Fraiji et. al.,[8] should provide the evidence for, or against, the hydrogen bond stabilization of the 2-AN:β-CD complex.

The complex formation of several other guest molecules with β- and TM-β-CD were investigated, as well. These fluorophores are anilinonaphthalenesulfonates and

were thoroughly studied by Catena and Bright.[7] In this experiment, fluorescence enhancement measurements were used to determine the binding constants, as well as thermodynamic factors for complexes involving 1-dimethylanilino-5-naphthalenesulfonamide (1,5-DNSA), 2-(*N*-methylanilino)naphthalene-6-sulfonic acid (2,6-MANS), and 2-(*p*-toluidinyl)naphthalene-6-sulfonic acid (2,6-TNS), Figure 2. Temperature dependence and pH studies were also performed.

Figure 2. Guest molecules used in fluorescence experiments.

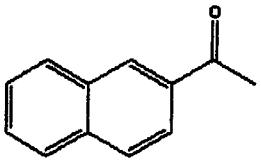

2-AN

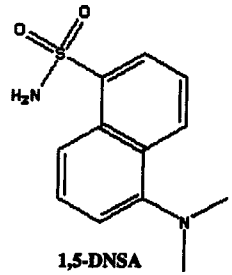

1,5-DNSA

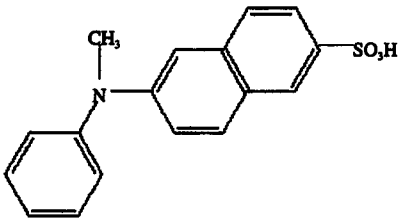

2,6-MANS

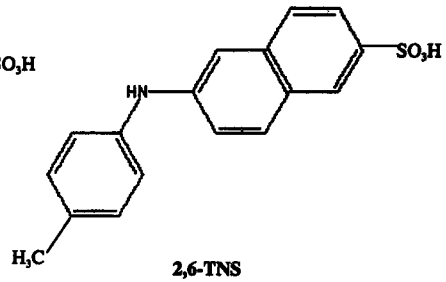

2,6-TNS

EXPERIMENTAL

A. 2-AN with TM-β -CD.

Solid 2-AN was received from Aldrich and dissolved in millipore water by stirring overnight. The absorbance of the stock solution at 340 nm was measured as 0.205 using a Hewlett-Packard 8452A diode array spectrophotometer. An accurately prepared stock solution of TM-β-CD near 0.01 M (Fluka, 1429.57 g/mol) was also prepared in millipore water. Next, a series of solutions were prepare [illegible] 00 mL volumetric flasks as described Table 1.

Table 1. 5.00 mL sample solutions of 2-AN in H_2O with TM-β-CD.

Solution	mL 2-AN stock in millipore H_2O*	mL 0.01 M TM-β-CD stock	[TM-β-CD] M	mL millipore H_2O
1	1.00	0.00	0.00	4.00
2	1.00	0.50	9.89×10^{-4}	3.50
3	1.00	1.00	1.98×10^{-3}	3.00
4	1.00	1.50	2.97×10^{-3}	2.50
5	1.00	2.00	3.96×10^{-3}	2.00
6	1.00	2.50	4.95×10^{-3}	1.50

*A 1:5 dilution of the 2-AN stock solution was performed and an absorbance of ~0.04 was measured for each solution. Absorbance values of ~0.01- 0.05 are most ideal for the fluorescence experiments.

To measure a binding constant (K) for the 2-AN:TM-β-CD complex, fluorescence intensities were then measured for solutions #1-6, along with a millipore water blank with a PTI Quantamaster spectrofluorometer. (Excitation = 340 nm; Emission = 370-500 nm; Slit widths = 4 nm; all spectra corrected.) Each solution was monitored with a thermocouple and allowed to reach 22 ± 0.1° C before being exposed to the intense beam of exciting light. The maximum fluorescence intensity and peak wavelength were recorded for each solution.

B. 2-AN with β-CD at high pH.

In order to study the binding of 2-AN to β-CD at high pH, a solution containing fixed amounts of 2-AN and β-CD was adjusted to increasingly higher pH values with NaOH. A stock solution of 2-AN was prepared in 0.010 M phosphate buffer (HPO_4^{2-}) and stirred overnight. The absorbance was measured as 0.171, and a 1:5 dilution of the 2-AN stock with 0.010 M phosphate buffer was performed. The pH of the solution was measured as 9.09 and a fluorescence spectrum was obtained. (Excitation = 340 nm; Emission = 370-500 nm; Slit widths = 4 nm; all spectra corrected; 22 ± 0.1° C.) Solid β-CD (Aldrich, 1135 g/mol) was added to give a concentration of 1.00 mM, and the fluorescence was measured once again. Concentrated NaOH was then added to the solution until a noticeable change in pH was obtained, the pH value was recorded, and the fluorescence was measured once again. Additonal NaOH was added and the fluorescence was measured until the pH reached 12.96. It is important to note that after each fluorescence scan, the sample was returned to the original 1:5 solution in order to avoid any volume changes.

The effect of pH on the 2-AN:β-CD complex was also studied by determining the K values at various concentrations of NaOH. A stock solution of 2-AN was prepared in 1.00 M NaOH, pH 13.46 and the absorbance at 340 nm was measured as 0.463. Also, a 0.0300 M β-CD stock solution was prepared using 1.0 M NaOH as the solvent. A series of sample solutions were then prepared as described in Table 2. The fluorescence of the sample solutions was measured and the data were recorded. (Excitation = 340 nm; Emission = 370-500 nm; Slit widths = 4 nm; all spectra corrected; 22 ± 0.1° C.) Trials were repeated a minimum of three times in order to obtain an average binding constant.

Table 2. 10.0 mL sample solutions of 2-AN in 1.00 M NaOH with β-CD.

Solution	mL 2-AN stock in 1.00 M NaOH*	mL 0.0300 M β-CD stock in 1.0 M NaOH	[β-CD] (M)	mL 1.00 M NaOH, pH 13.46 **
1	1.00	0.00	0.00	9.00
2	1.00	1.00	3.00×10^{-3}	8.00
3	1.00	2.00	6.00×10^{-3}	7.00
4	1.00	4.00	1.20×10^{-2}	5.00
5	1.00	6.00	1.80×10^{-2}	3.00
6	1.00	8.00	2.40×10^{-2}	1.00

*A 1:10 dilution of the 2-AN stock solution was performed for an absorbance of ~0.05 for each solution.
**1.00 M NaOH, pH 13.46 for all solutions.

Additional sets of solutions were prepared for several other pH values, as well. However, a variety of experimental problems, including CD aggregation, required slight modifications to solution preparation. Tables 3-7 summarize the directions used in making the different solutions. The NaOH concentrations and pH values were a result of contributions from each of the 2-AN, β–CD, and NaOH stock solutions. Ultimately, the results were recorded for 0.190 M NaOH, pH12.88; 0.110 M NaOH, pH 12.11; 0.0100 M NaOH, pH 11.87; 1.00 mM NaOH, pH 10.82; and millipore water, pH ~7.00. The fluorescence was measured for each set of solutions and trials were repeated in triplicate for an average binding constant.

Table 3. 10.0 mL sample solutions of 2-AN in 0.190 M NaOH with β-CD.

Solution	mL 2-AN stock in 1.00 M NaOH*	mL 0.0150 M β-CD stock in 0.100 M NaOH	[β-CD] (M)	mL 0.100 M NaOH, pH 12.88 **
1	1.00	0.00	0.00	9.00
2	1.00	1.00	1.50×10^{-3}	8.00
3	1.00	2.00	3.00×10^{-3}	7.00
4	1.00	4.00	6.00×10^{-3}	5.00
5	1.00	6.00	9.00×10^{-3}	3.00
6	1.00	8.00	1.20×10^{-2}	1.00

*A 1:10 dilution of the 2-AN stock solution was performed for an absorbance of ~0.05 for each solution.
**0.190 M NaOH, pH 12.88 for all solutions.

Table 4. 10.0 mL sample solutions of 2-AN in 0.110 M NaOH with β-CD.

Solution	mL 2-AN stock in 1.00 M NaOH*	mL 0.0150 M β-CD stock in 0.010 M NaOH	[β-CD] (M)	mL 0.010 M NaOH, pH 12.11 **
1	1.00	0.00	0.00	9.00
2	1.00	1.00	1.50×10^{-3}	8.00
3	1.00	2.00	3.00×10^{-3}	7.00
4	1.00	4.00	6.00×10^{-3}	5.00
5	1.00	6.00	9.00×10^{-3}	3.00
6	1.00	8.00	1.20×10^{-2}	1.00

*A 1:10 dilution of the 2-AN stock solution was performed for an absorbance of ~0.05 for each solution.
** 0.110 M NaOH, pH 12.11 for all solutions.

Table 5. 10.0 mL sample solutions of 2-AN in 0.010 M NaOH with β-CD.

Solution	mL 2-AN stock in 0.0100 M NaOH*	mL 0.0150 M β-CD stock in 0.010 M NaOH	[β-CD] (M)	mL 0.010 M NaOH, pH 11.87 **
1	1.00	0.00	0.00	9.00
2	1.00	0.500	7.50×10^{-4}	8.50
3	1.00	1.00	1.50×10^{-3}	8.00
4	1.00	2.00	3.00×10^{-3}	7.00
5	1.00	4.00	6.00×10^{-3}	5.00
6	1.00	6.00	9.00×10^{-3}	3.00

*A 1:10 dilution of the 2-AN in 0.0100 M NaOH stock solution (A = 0.231) was performed for an absorbance of ~0.02 for each solution.
**0.010 M NaOH, pH 11.87 for all solutions.

Table 6. 10.0 mL sample solutions of 2-AN in 1.00 mM NaOH with β-CD.

Solution	mL 2-AN stock in 0.0100 M NaOH*	mL 0.0150 M β-CD stock in 1.00 mM NaOH	[β-CD] (M)	mL 1.00 mM NaOH, pH 10.82 **
1	1.00	0.00	0.00	9.00
2	1.00	0.500	7.50×10^{-4}	8.50
3	1.00	1.00	1.50×10^{-3}	8.00
4	1.00	1.50	2.25×10^{-3}	7.50
5	1.00	2.00	3.00×10^{-3}	7.00
6	1.00	3.00	4.50×10^{-3}	6.00
7	1.00	4.00	6.00×10^{-3}	5.00
8	1.00	6.00	9.00×10^{-3}	3.00

*A 1:10 dilution of the 2-AN in 1.00 mM NaOH stock solution (A = 0.371) was performed for an absorbance of ~0.04 for each solution.
**1.00 M NaOH, pH 10.82 for all solutions.

Table 7. 10.0 mL sample solutions of 2-AN in H_20 with β-CD.

Solution	mL 2-AN stock in millipore H_20*	mL 5.00 mM β-CD stock in H_2O	[β-CD] (M)	mL millipore H_20 **
1	1.00	0.00	0.00	9.00
2	1.00	0.500	2.50×10^{-4}	8.50
3	1.00	1.00	5.00×10^{-4}	8.00
4	1.00	2.00	1.00×10^{-3}	7.00
5	1.00	4.00	2.00×10^{-3}	5.00
6	1.00	6.00	3.00×10^{-3}	3.00

*A 1:10 dilution of the 2-AN in H_20 stock solution (A = 0.205) was performed for an absorbance of ~0.04 for each solution.
**pH ~7.0 for all solutions.

C. 1,5-DNSA with β-CD.

1,5-DNSA was received from Aldrich. An amount fitting on the tip of a small spatula was used to make a ~75 mL stock solution in millipore water. The absorbance at 320 nm was measured as A = 0.135. A 0.005 M β–CD stock solution and a fixed amount of 0.1 M phosphate buffer, pH 7.00 were used in the preparation of sample solutions described in Table 8.

Fluorescence enhancement measurements were then collected with the sample solutions. (Excitation = 320 nm; Emission = 400-770 nm; Slit widths = 4 nm; all spectra corrected; 22 ± 0.1° C.) Also, in order to limit the effects of a second order peak, a filter (thick glass square) was placed before the emission monochrometer.

Table 8. 10.0 mL sample solutions of 1,5-DNSA in H_20 with β-CD.

Solution	mL 1,5-DNSA stock in millipore H_20*	mL 0.100 M phosphate buffer, pH 7.00	mL 5.00 mM β-CD stock in H_2O	[β-CD] (M)	mL millipore H_20
1	1.00	1.00	8.00	4.00×10^{-3}	0.00
2	1.00	1.00	6.00	3.00×10^{-3}	2.00
3	1.00	1.00	4.00	2.00×10^{-3}	4.00
4	1.00	1.00	2.00	1.00×10^{-3}	6.00
5	1.00	1.00	1.00	5.00×10^{-4}	7.00
6	1.00	1.00	0.00	0.00	8.00

*A 1:10 dilution of the 1,5-DNSA in H_20 stock solution was performed for an absorbance of ~0.013 for each solution.

D. 1,5-DNSA with TM-β-CD.

Complex formation between 1,5-DNSA and TM-β-CD was also investigated. Table 8 was followed for sample preparation with a 5.00 mM TM-β-CD stock. Fluorescence enhancement measurements were done in triplicate and peak intensities, as well as the integrated peak areas, were recorded.

E. 2,6-MANS with TM-β-CD.

2,6-MANS was ordered from Molecular Probes. A stock solution in 0.100 M phosphate buffer, pH 7.00 was prepared and the absorbance at 316 nm was measured as 0.801. A stock solution of 0.0250 M TM-β-CD, and a set of sample solutions were prepared as described in Table 9. Fluorescence enhancement measurements were then performed in triplicate, and the data were recorded. (Excitation = 320 nm; Emission = 360-770 nm; Slit widths = 4 nm; all spectra corrected; 24.5 ± 0.1° C.) The sample solutions were also used to collect fluorescence data at a series of additional temperatures, (18°C, 32°C, and 40°C, ± 0.1° C).

Table 9. 10.0 mL sample solutions of 2,6-MANS in 0.100 M phosphate buffer, pH 7.00 with TM-β-CD.

Solution	mL 2,6-MANS in 0.100 M phosphate buffer*	mL 0.0250 M TM-β-CD stock in H_2O	[TM-β-CD] (M)	mL millipore H_2O
1	1.00	8.00	0.0100	1.00
2	1.00	2.00	2.50×10^{-3}	7.00
3	1.00	0.50	6.25×10^{-4}	8.50
4	1.00	0.125	1.56×10^{-4}	8.875
5	1.00	0.3125	3.90×10^{-5}	8.969
6	1.00	0.00	0.00	9.00

*A 1:10 dilution of the 2,6-MANS in 0.100 M phosphate buffer, pH 7.00 stock solution was performed for an absorbance of ~0.08 for each solution.

F. 2,6-MANS with more concentrated TM-β–CD.

Additional experimentation with more concentrated CD sample solutions was also performed in order to observe any evidence of a 2:1 complex system. The 2,6-MANS in 0.100 M phosphate buffer stock solution, along with a 0.025 M stock solution of TM-β-CD, were used in the sample preparation described in Table 10. Fluorescence enhancement measurements were then collected and recorded. (Excitation = 320 nm; Emission = 360-770 nm; Slit widths = 4 nm; all spectra corrected; 24.5± 0.1° C.)

Table 10. 5.00 mL sample solutions of 2,6-MANS in 0.100 M phosphate buffer, pH 7.00 with TM-β-CD.

Solution	mL 2,6-MANS in 0.100 M phosphate buffer*	mL 0.0250 M TM–β-CD stock in H_2O	[TM-β-CD] (M)	mL millipore H_2O
1	1.00	4.00	0.0200	0.00
2	1.00	3.50	0.0175	0.50
3	1.00	3.00	0.0150	1.00
4	1.00	2.50	0.0125	1.50
5	1.00	2.00	0.0100	2.00
6	1.00	0.00	0.00	4.00

*A 1:10 dilution of the 2,6-MANS in 0.100 M phosphate buffer, pH 7.00 stock solution was performed for an absorbance of ~0.08 for each solution.

G. pH studies with 2,6-TNS.

pH studies were performed with 2,6-TNS (Fluka) to ensure that the pKa of the fluorophore was not in a close proximity to the pH ~7.0 of the buffer. In these studies, the absorbance was measured as a function of pH. The absorbance was measured after each small addition of 1 M HCl to a stock solution of 2,6-TNS in 0.010 M phosphate buffer. A range of pH 8.41 - 1.59 was investigated. It is important to note that after each absorbance measurement, the sample volume was returned to the stock solution in order to avoid any volume changes.

H. 2,6-TNS with TM-β-CD.

Fluorescence enhancement studies were performed with 2,6-TNS and TM-β-CD in water. A 6.32×10^{-5} M 2,6-TNS in 250 mL millipore H_20 stock solution was prepared and the absorbance was measured as 1.12. A 0.0125 M TM-β-CD stock solution was also prepared. A set of sample solutions was prepared as described in Table 11. Fluorescence enhancement measurements were collected and recorded in triplicate in order to obtain an average binding constant. (Excitation = 320 nm; Emission = 360-770 nm; Slit widths = 4 nm; all spectra corrected; 25 ± 0.1°C.)

Table 11. 10.0 mL sample solutions of 2,6-TNS in millipore H_20 with TM-β-CD.

Solution	mL *diluted* 2,6-TNS in H_20 stock*	mL 0.0125 M TM-β-CD stock in H_2O	[TM-β-CD] (M)	mL millipore H_20
1	1.00	0.500	6.25×10^{-4}	0.00
2	1.00	0.250	3.13×10^{-4}	0.50
3	1.00	0.125	1.56×10^{-4}	1.00
4	1.00	0.0625	7.80×10^{-5}	1.50
5	1.00	0.03125	3.90×10^{-5}	2.00
6	1.00	0.00	0.00	4.00

*A 1:2 dilution of the 2,6-TNS in H_20 stock solution was performed. The sample solutions were then made from the diluted stock for an absorbance of ~0.06 for each solution.

RESULTS

A. 2-AN with TM-β-CD.

The fluorescence scans for solutions #1-6 of Table 1 are included in Figure 3. The solutions had a maximum fluorescence intensity at about 432 nm which decreased in intensity as the concentration of TM-β-CD increased. Assuming a 1:1 fluorophore to CD stoichiometry, and using a modified version of the Stern-Volmer equation, the binding constant was then determined using Eq. 1.

$$F^{\circ}/F = 1 + K[Q], \qquad (1)$$

where F° is the fluorescence in the absence of quencher, F is the fluorescence in the presence of quencher, K is the binding constant, and Q is the concentration of CD quencher. All fluorescence measurements were corrected for solvent background. Upon constructing a plot of F°/F vs. [CD], we can determine K from the slope. The slope and, therefore, binding constant of the Stern-Volmer plot for the 2-AN:TM-β-CD complex was 131 M^{-1}. An R^2 value of > 0.99 was obtained, indicating good linearity.

B. 2-AN with β-CD at high pH.

The effect of high pH on the binding of 2-AN to a fixed concentration of β-CD was first studied using phosphate buffer. The fluorescence intensities are displayed in Figure 4. As the number of the scan increases, the pH of the solution increases, as well. The experiment was not conclusive because at the maximum pH (12.96), a significant number of hydroxyl groups remain protonated on the CD rim. In order to draw any conclusions, a larger pH value must be achieved.

Figure 3. 2-AN with TM-β-CD.

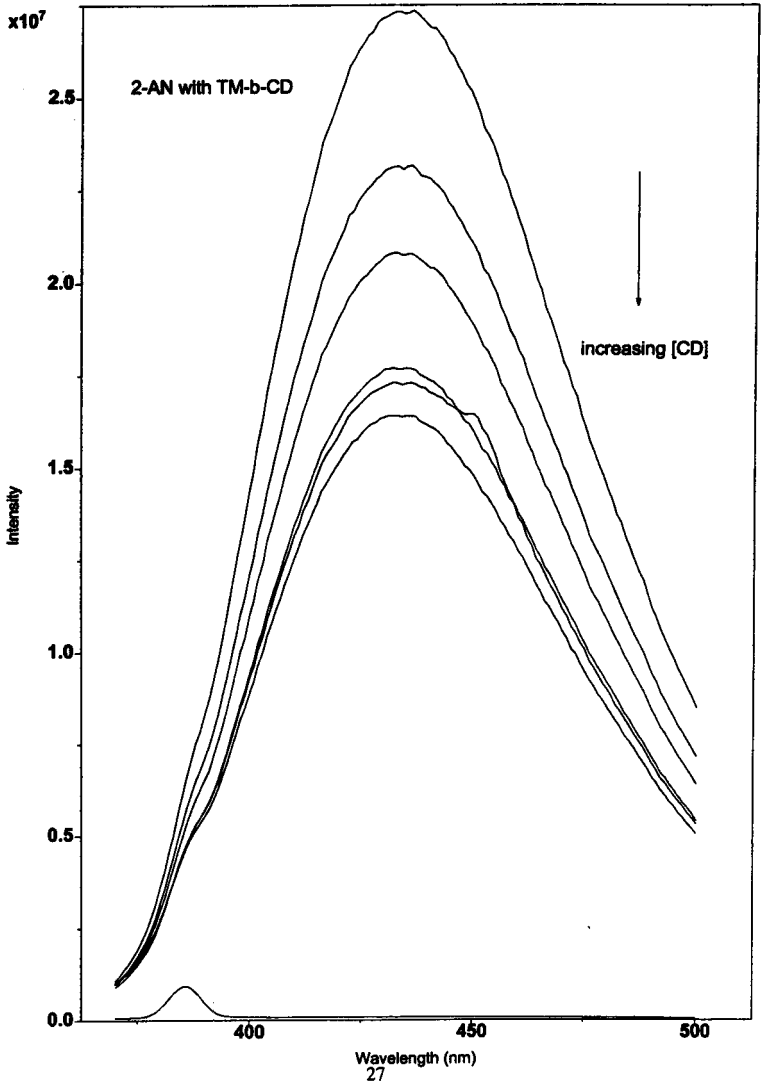
x10^7
2-AN with TM-b-CD
increasing [CD]
Intensity
2.5
2.0
1.5
1.0
0.5
0.0
400
450
500
Wavelength (nm)

Figure 4. 2-AN with β-CD at high pH. 1. pH = 9.09; 2. pH = 8.99; 3. pH = 10.42; 4. pH = 12.01; 5. pH = 12.21; 6. pH = 12.50; 7. pH = 12.82; 8. pH =12.96.

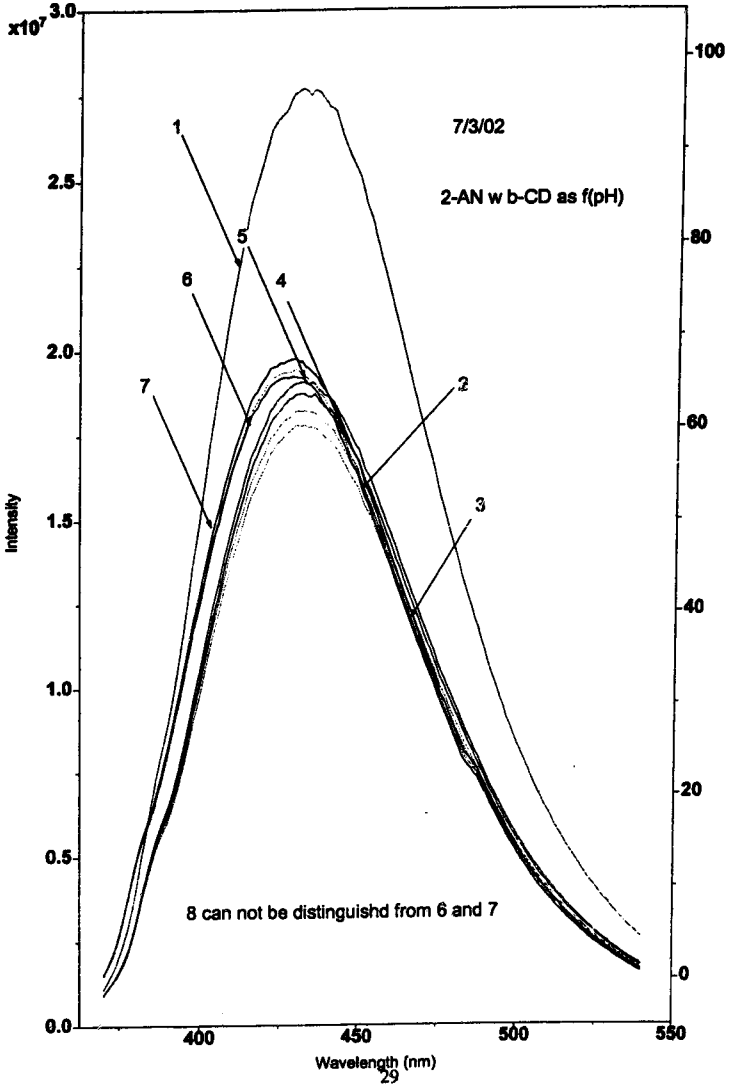
x10^7
3.0
2.5
2.0
1.5
1.0
0.5
0.0
Intensity
100
80
60
40
20
0
400
450
500
550
Wavelength (nm)
7/3/02
2-AN w b-CD as f(pH)
1
2
3
4
5
6
7
8 can not be distinguishd from 6 and 7

The results of the higher pH measurements, using NaOH to adjust the pH, are included in Figure 5, Table 12, and Figure 6. In these fluorescence quenching experiments, the concentration of 2-AN was fixed while the β-CD concentration varied in a set of solutions, each at a particular pH. Figure 5 shows the data for solutions in 1.00 M NaOH, pH 13.46. The fluorescence intensities are quenched as CD concentration increases. Figure 5 is representative of the results observed at all other pH values. The modified Stern-Volmer equation was used and F°/F vs. [CD] was plotted for each set of trials at the different pH values. Table 12 reports the average binding constants, K, for each of the pH values studied. These results were used to construct a plot of K vs. pH in Figure 6.

Figure 5. 2-AN with β-CD , pH 13.46.

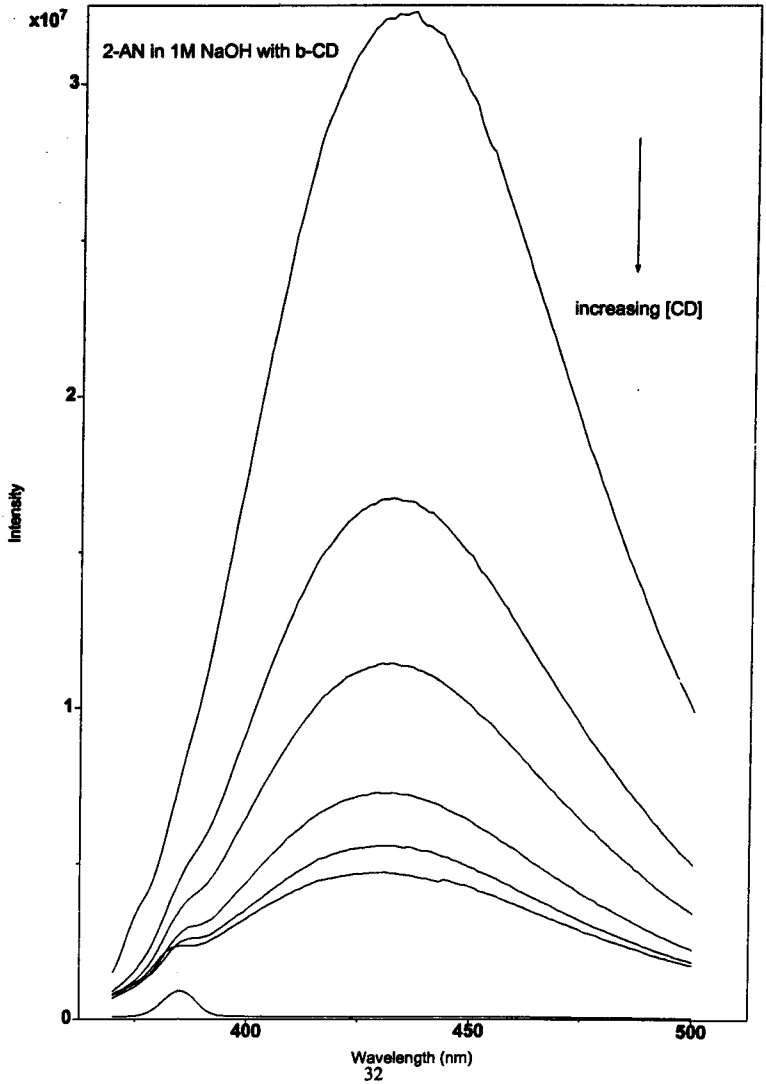
x10^7
2-AN in 1M NaOH with b-CD
3
2
1
0
Intensity
increasing [CD]
400
450
500
Wavelength (nm)

Table 12. Binding constants at high pH.

pH	K (M^{-1})
13.46	276 ± 22
12.88	285 ± 9
12.11	324 ± 30
11.87	405 ± 29
10.82	445 ± 19
~7.00	581 ± 6*

* Catena, G.C., Bright, F.V. *Anal. Chem.* 1989, 61, 915.

Figure 6. Binding constant vs. pH of the 2-AN:β-CD complex.

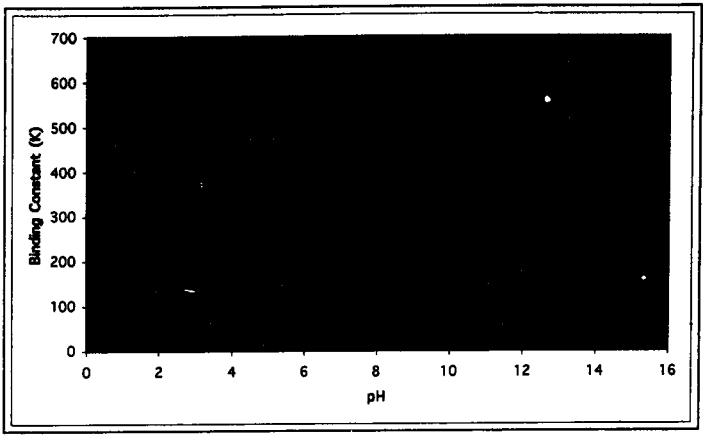
Binding Constant (K)
700
600
500
400
300
200
100
0
0
2
4
6
8
10
12
14
16
pH

C. 1,5-DNSA with β–CD.

The results of the fluorescence enhancement measurements for the 1,5-DNSA:β-CD complex formation are included in Figure 7. As the concentration of CD increased, the fluorescence intensities increased. Also, a slight blue shift in peak maximum (~10 nm) was noted with higher concentrations of β-CD.

In order to determine the binding constant, a double-reciprocal plot was constructed. In the case of a 1:1 stoichiometry between a fluorophore (Fl) and a CD, the equilibrium expression can be written as follows,

$$Fl + CD = Fl{:}CD \quad \text{and} \qquad (2)$$

$$K = [Fl{:}CD] / [Fl]\,[CD], \qquad (3)$$

where [Fl:CD] is the fluorophore:CD complex. If $[Fl]_o$ is the total concentration of fluorophore, then $[Fl]_o = [Fl] + [Fl{:}CD]$. We can write the complex concentration as $[Fl{:}CD]_\infty$, when [CD] is infinite and all of the Fl is bound in complex form. We can then write Eq. 4.

$$[Fl{:}CD]/[Fl]_o = [Fl{:}CD]/[Fl{:}CD]_\infty = K[CD]/1+K[CD] \qquad (4)$$

Furthermore, the complex concentration can be related to the fluorescence signal in Eq. 5.

$$[Fl{:}CD] = k\,(F - F_o) \qquad (5)$$

where F is the measured fluorescence at a given [CD], F_o is the measured fluorescence when [CD] = 0, and k is the proportionality constant between concentration and fluorescence intensity. Thus, $[Fl{:}CD]_\infty = k\,(F_\infty - F_o)$, where F_∞ represents the fluorescence when all of the fluorophore is bound, the limiting fluorescence. Let $\Delta F = (F - F_o)$ and $\Delta F_\infty = (F_\infty - F_o)$ and plug Eq. 5 into Eq. 4.

$$\Delta F/\Delta F_\infty = K[CD]/1+K[CD] \qquad (6)$$

Rearrange Eq. 6 and divide through by [CD], and then by ΔF, gives Eq. 7.

$$1/\Delta F = 1/([CD]K\Delta F + 1/\Delta F_\infty \qquad (7)$$

A plot of $1/\Delta F$ vs. $1/[CD]$ has a slope equal to $1/(\Delta F_\infty K)$ and a y-intercept equal to $1/\Delta F_\infty$. Thus, slope/intercept gives the binding constant, K.

A double-reciprocal plot for the 1,5-DNSA:β-CD data resulted in a binding constant of 151 M^{-1}, and an R^2 value > 0.99.

D. 1,5-DNSA with TM-β-CD.

Fluorescence enhancement measurements of 1,5-DNSA with TM-β-CD are shown in Figure 8. Again, the fluorescence intensity increased with increasing concentrations of CD, and there was a slight blue shift in peak heights (~10 nm) at the higher concentrations of CD. A double-reciprocal plot was constructed for each of the trials and an average K of 105 ± 29 M^{-1} was calculated.

Figure 7. 1,5-DNSA with β-CD.

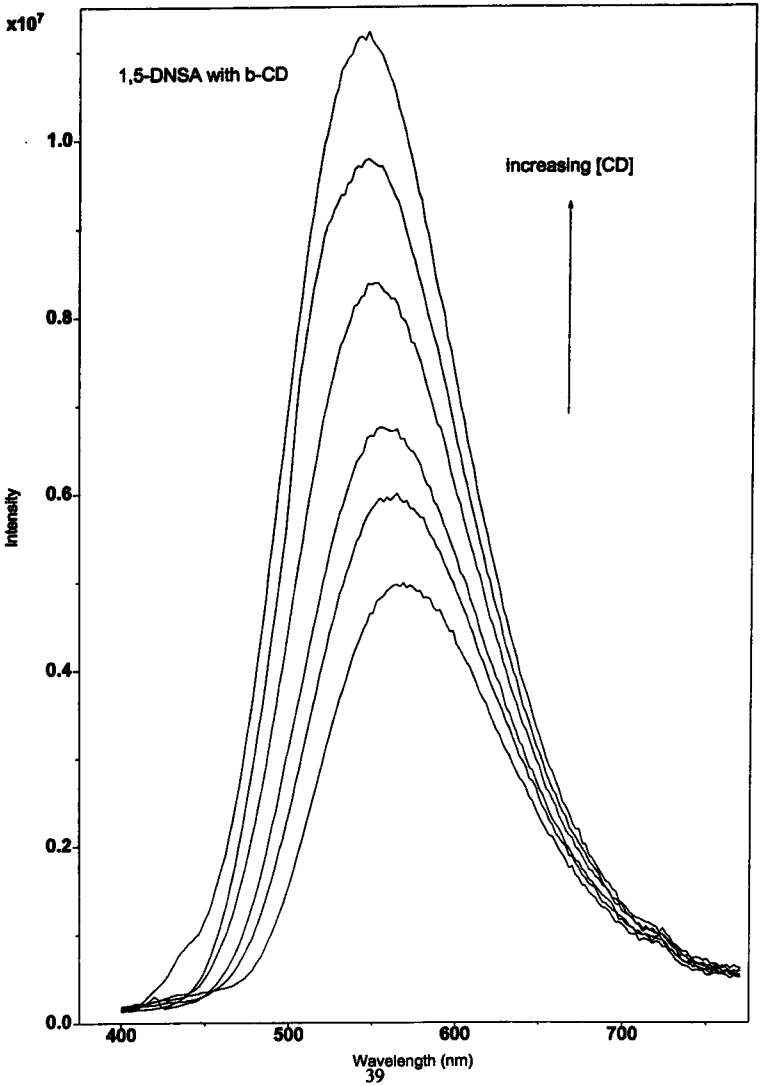
x10^7
1,5-DNSA with b-CD
increasing [CD]
1.0
0.8
0.6
0.4
0.2
0.0
Intensity
400
500
600
700
Wavelength (nm)

Figure 8. 1,5-DNSA with TM-β-CD.

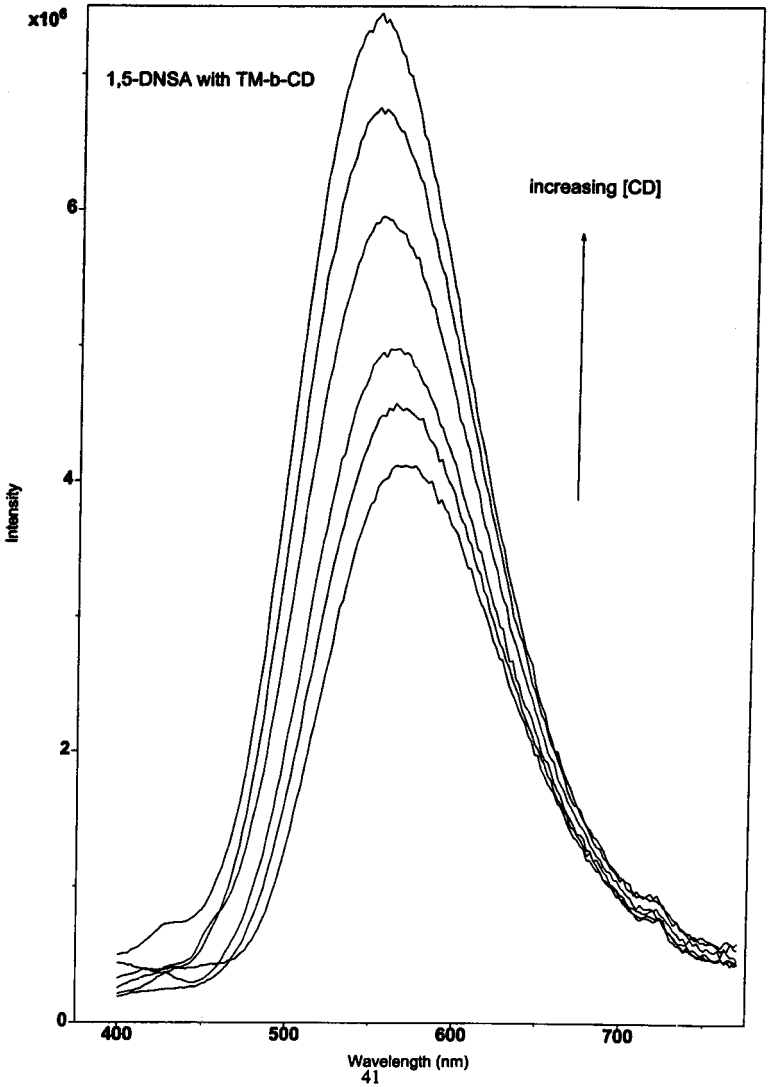
x10^6
1,5-DNSA with TM-b-CD
increasing [CD]
6
4
2
0
Intensity
400
500
600
700
Wavelength (nm)

E. 2,6-MANS with TM-β-CD.

The results of the fluorescence intensity experiments with 2,6-MANS and TM-β-CD are included in Figure 9. These spectra were collected at 25 °C. The same general trend was obtained at each of the additional temperatures used for the experiment. The fluorescence data were used to construct a double-reciprocal plot and to determine K. The binding constant was also determined using both Mathematica and Excel Statistical Data Analysis programs.[13] These programs fit the data by a non-linear regression method. Eq. 6 can be rewritten as Eq. 8, which was used for the non-linear regression fits.

$$\Delta F/\Delta F_\infty = K[CD]/1+K[CD] \qquad (6)$$

$$\Delta F = (\Delta F_\infty K\,[CD])/1 + K\,[CD] \qquad (8)$$

Table 13 contains the K values and uncertainties for each of the methods described. The initial guesses used for the non-linear regression methods were obtained from the linear, double-reciprocal plots. These non-linear data are more accurate and agree nicely for both methods.

The thermodynamic parameters were then determined using the two well-known expressions for Gibb's Free Energy.

$$\Delta G^\circ = -RT\ln(K) \qquad (9)$$

$$\Delta G^\circ = \Delta H^\circ - T\Delta S^\circ \qquad (10)$$

where G is the free energy, R is the gas constant, T is the standard-state temperature, K is the equilibrium constant, H is the enthalpy, and S is the entropy of the system. Eq. 9 can then be set equal to Eq 10 and rewritten to give Eq. 11.

$$\ln(K) = -\Delta H^\circ/RT + \Delta S^\circ/R \quad (11)$$

Finally, using the calculated K values, a van't Hoff plot of ln(K) vs. 1/T was constructed to determine the enthalpy and entropy parameters. Figure 10 shows the van't Hoff plot for the non-linear methods. Using Eq. 11, ΔH and ΔS were calculated as -35 ± 3 kJ/mol and -47 ± 8 J/mol K, respectively.

F. 2,6-MANS with more concentrated TM-β-CD.

In order to investigate any formation of a 2:1, TM-β-CD:2,6-MANS complex, the concentration of CD was increased up to 0.02 M. Figure 11 shows the fluorescence spectra at these higher concentrations of CD maintained at 25 °C. No significant change in intensity or peak maximum was observed and the probability of a 2:1 complex was eliminated.

Figure 9. 2,6-MANS with TM-β-CD.

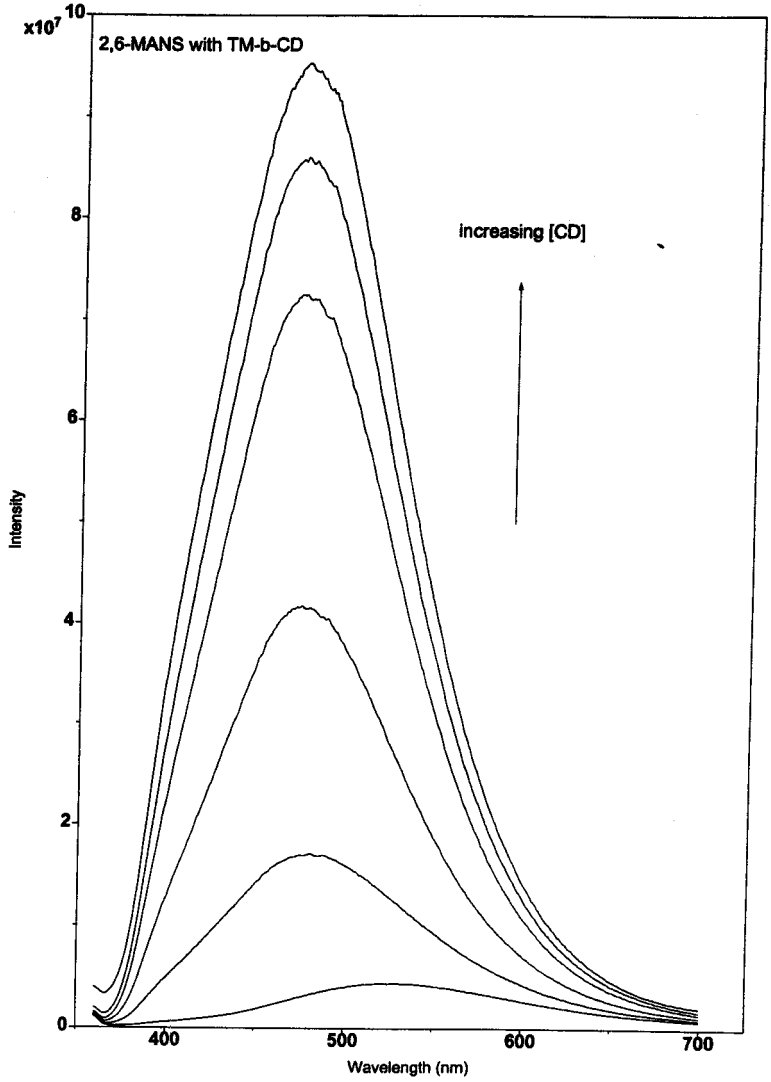
x10^7
10
2,6-MANS with TM-b-CD
8
increasing [CD]
6
Intensity
4
2
0
400
500
600
700
Wavelength (nm)

Table 13. Average binding constants (M^{-1}) using linear and non-linear fits.

Temp	Excel linear plot	Mathematica Non-linear Regression	Excel Non-linear Regression
18 °C	5619 ± 196	5991 ± 90	5991 ± 90
25 °C	4767 ± 302	4797 ± 408	4802 ± 408
32 °C	3162 ± 33	3435 ± 127	3435 ± 127
40 °C	2085 ± 165	2444 ± 194	2444 ± 194

Figure 10. van't Hoff plot.

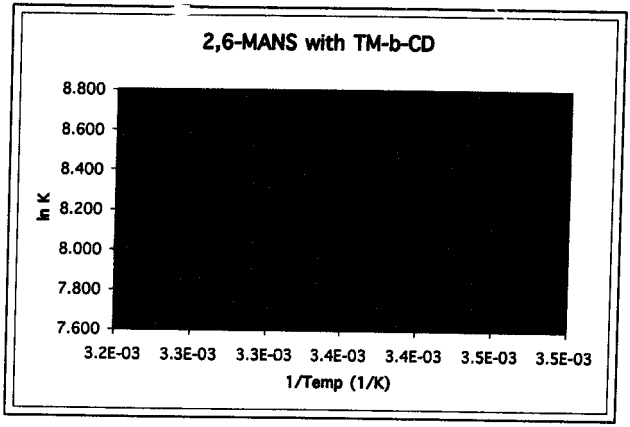
2,6-MANS with TM-b-CD
8.800
8.600
8.400
8.200
8.000
7.800
7.600
ln K
3.2E-03
3.3E-03
3.3E-03
3.4E-03
3.4E-03
3.5E-03
3.5E-03
1/Temp (1/K)

Figure 11. 2,6-MANS with more concentrated TM-β-CD.

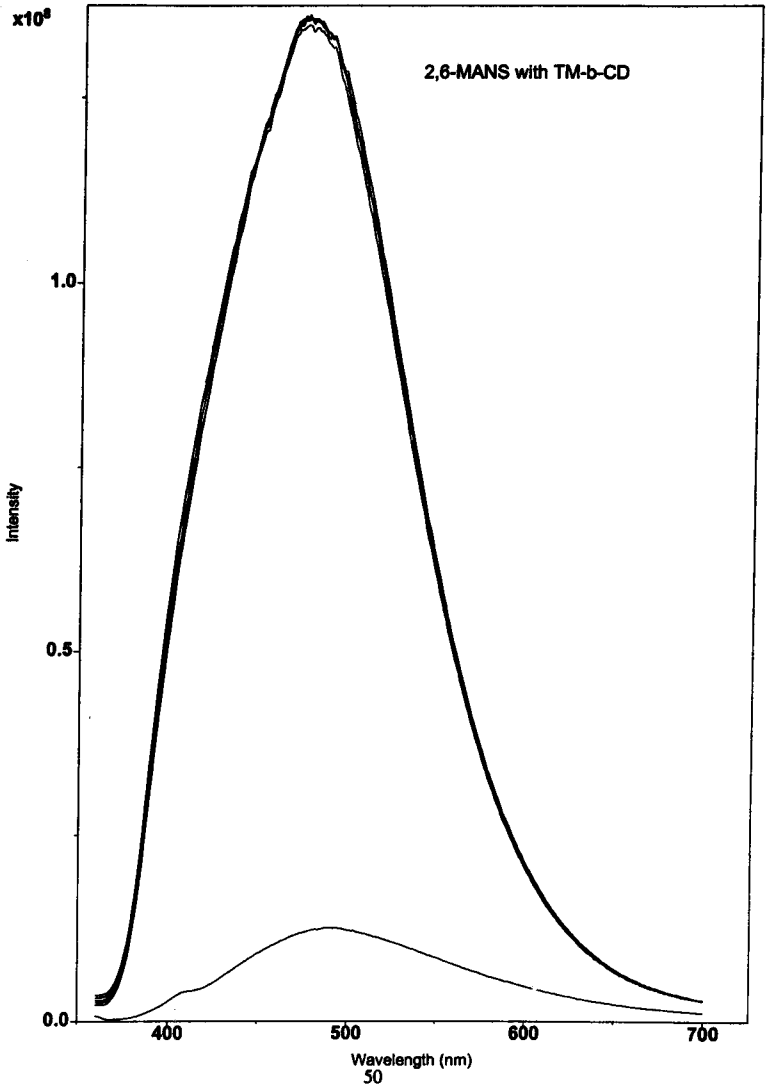
x10⁶
2,6-MANS with TM-b-CD
1.0
0.5
0.0
Intensity
400
500
600
700
Wavelength (nm)

G. pH studies with 2,6-TNS.

A pH of ~7.00 was determined adequate for fluorescence studies with 2,6-TNS; that is, only one ionization form of 2,6-TNS was present at pH 7.00. The overlapped spectra at several pH values are included in Figure 12. Over the pH range of 8.41 – 1.59, there was no significant change in the absorption spectrum. The pKa of the amine group is, therefore, less than 1.59. It seems that each of the aromatic regions of the 2,6-TNS pull electron density away from the amine group, making it very acidic. Thus, it is safe to carry out the fluorescence studies using a phosphate buffer of pH ~7.00 since only one ionization form of 2,6-TNS would be present.

H. 2,6-TNS with TM-β-CD.

The results of the fluorescence studies performed with 2,6-TNS and TM-β-CD are represented in Figure 13. There was no observed shift in peak maxima relative to water. The data were used to construct a double-reciprocal plot in order to determine the binding constant. K was calculated as $2100 \pm 46\ M^{-1}$. Mathematica and Excel non-linear regression methods were also used and resulted in a K of $2358 \pm 124\ M^{-1}$ for each fit.

Figure 12. pH studies with 2,6-TNS.

Overlaid Sample Spectra

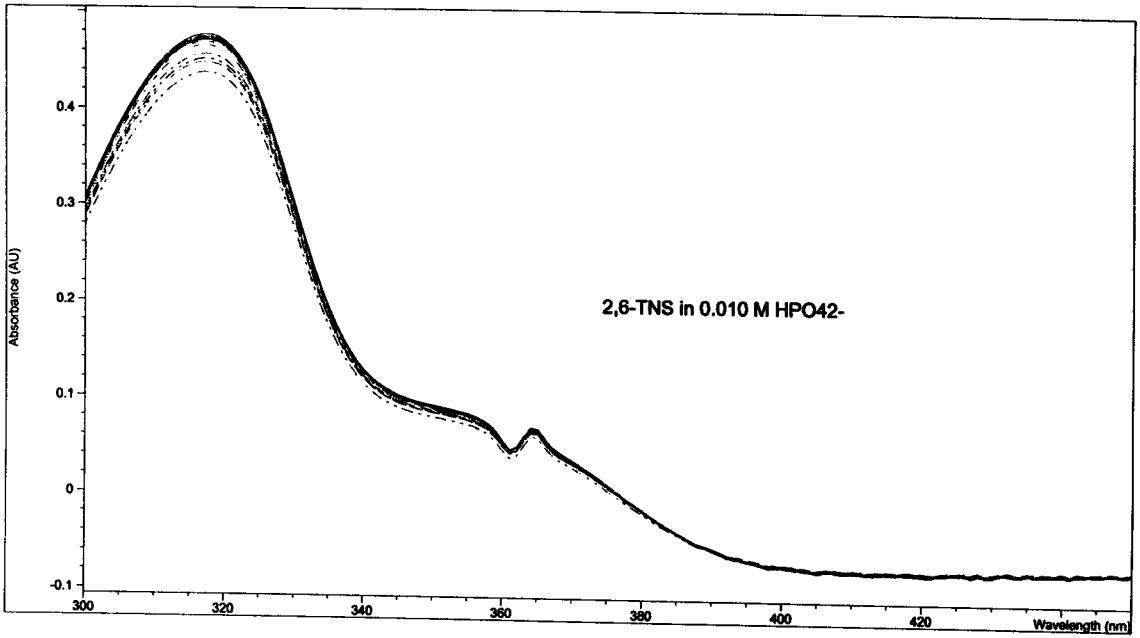

*** End ***

Figure 13. 2,6-TNS with TM-β-CD.

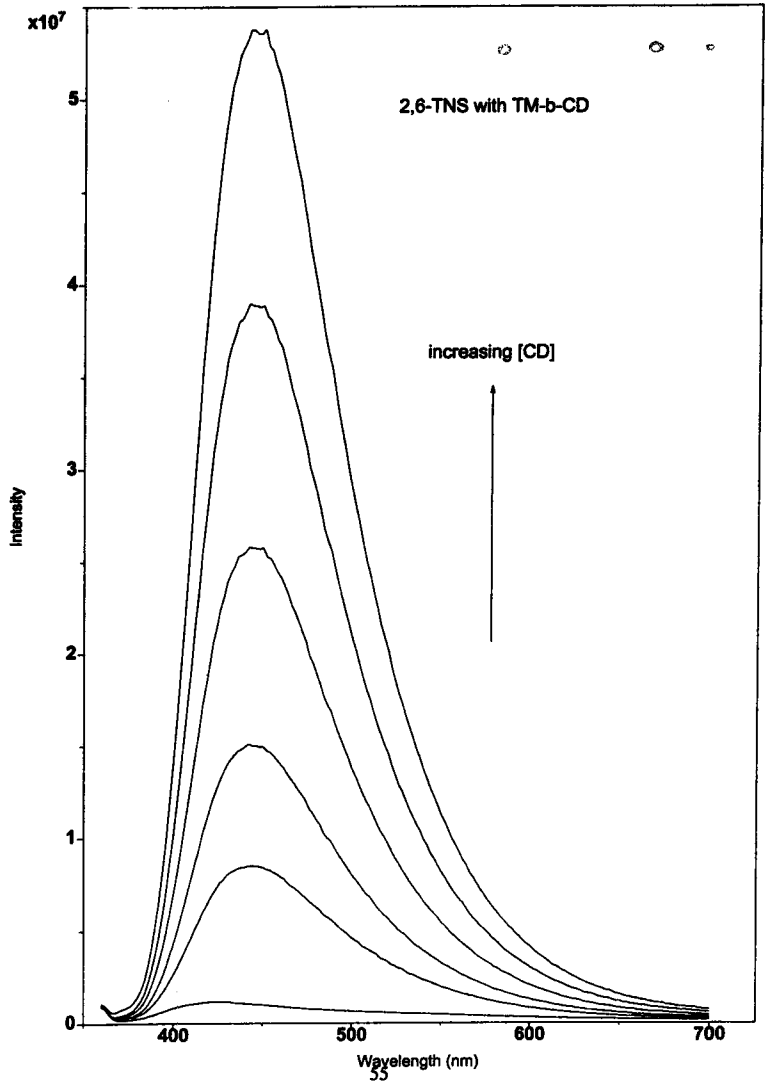
x10^7
5
4
3
2
1
0
Intensity
2,6-TNS with TM-b-CD
increasing [CD]
400
500
600
700
Wavelength (nm)

DISCUSSION

I. 2-AN with TM-β-CD.

The binding constant of 2-AN with TM-β-CD was measured in order to better understand the stabilizing effects of the 2-AN:β-CD complex. The K value for the β-CD complex was reported as 581 M^{-1}.[8] Fraiji et. al. also measured K for 2-AN with dimethyl-β-cyclodextrin (DM-β-CD). An average of fourteen out of the total twenty-one β-CD rim hydroxyl groups are converted to $-OCH_3$ groups in DM-β-CD. Methylation generally occurs at the second and sixth position –OH groups, leaving the hydroxyl group at the third position available for hydrogen bonding. If hydrogen bonding plays a significant role in stabilizing the 2-AN:β-CD complex, then the binding constant should decease in the absence of CD rim -OH groups. However, K significantly increases to 1048 M^{-1} for the DM-β-CD complex.[8] DM-β-CD has both a more hydrophobic cavity, due to the methyl groups, as well as hydrogen bonding capability with the -OH groups at position three of the wide rim. Each of these stabilizing effects contribute to the large binding constant. After complete methylation of the CD rim -OH groups, as with TM-β-CD, the binding constant decreased significantly to 131 M^{-1}. It is unclear, however, whether this drastic decrease in K is due to steric factors, the loss of hydrogen binding, or both.

Ealing space filling models provided some insight into the factors that could destabilize the 2-AN:TM-β-CD complex. Since the $-OCH_3$ groups are significantly larger than the -OH groups on the β-CD rim, the cavity opening is more crowded, which may hinder complex formation. However, the models show that the naphthalene portion

UN82 IANNACONE, JAMIE M. THE USE OF FLUORESCENCE TO ETC.
I11u/2003 CHEMISTRY HRS. 6/03 2-2

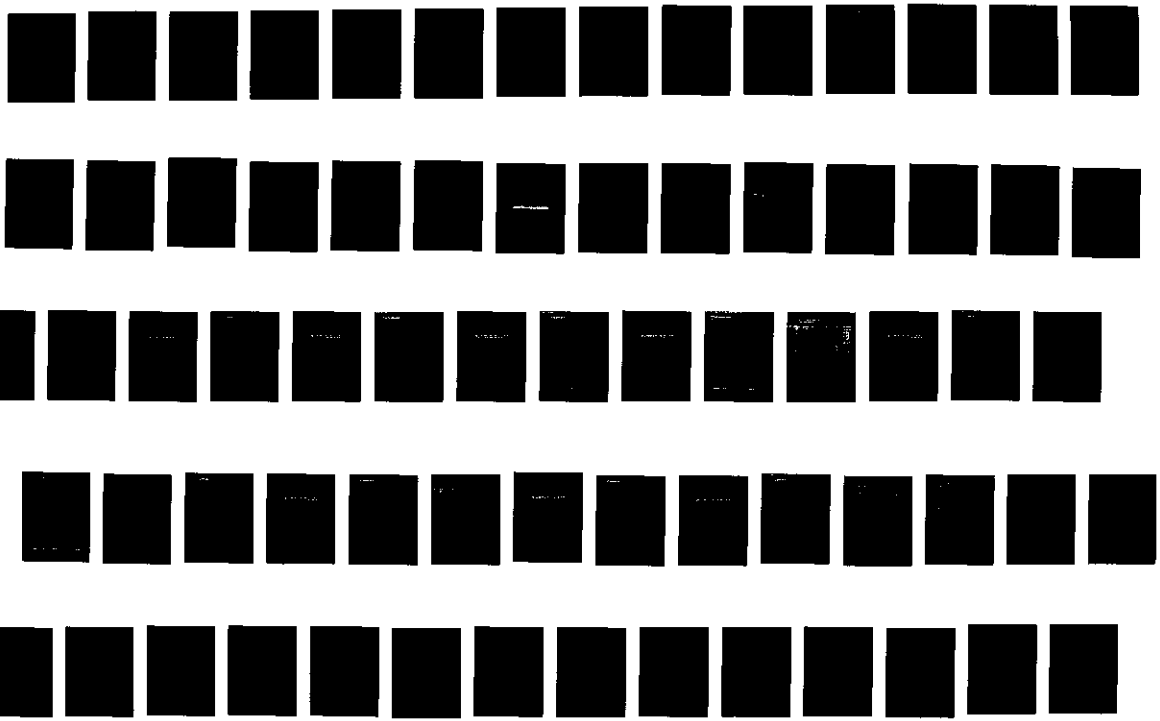

of the 2-AN molecule can fit inside the TM-β-CD cavity. This suggests that the destabilized complex is not a result of steric effects alone.

The 2-AN:TM-β-CD complex cannot be stabilized by hydrogen bonding, as could be the case for the 2-AN:β-CD complex. To investigate the importance of hydrogen bonding in complex formation, we studied the binding of 2-AN to β-CD at high pH. NaOH was added to the samples to yield solutions at high pH environments. The corresponding K values are listed in Table 12. As the pH is increased from a value of ~7.00 to 13.46, the K value decreases from 581 M^{-1} to near half this value (276 M^{-1}). Figure 6 shows the trend of the binding constant versus pH.

The most basic solution included in Figure 6 had a pH of 13.46. This particular pH is above the pKa associated with the -OH groups at the second and third positions of the β-CD rim (~12.2), causing these groups to become deprotonated and to lose their hydrogen bond capabilities.[11] However, this pH value does not quite reach the pKa for the -OH group at the sixth position (~15-16), leaving it protonated.[11] Furthermore, Figure 6 shows an inflection point at about pH 12.5. The decrease in K is, therefore, most significantly due to the loss of hydrogen bond capability at the second and third positions. It is these groups that interact with the carbonyl oxygen of the 2-AN guest molecule and play a major role in stabilizing the complex.

Although we attribute hydrogen bonding as the most significant stabilizing affect of the 2-AN:β-CD complex, there remains some reason to include possible steric contributions. The binding constant for the 2-AN:β-CD complex at high pH (276 M^{-1}) is still much larger than K for the TM-β-CD complex (131 M^{-1}). The methyl substituents of

the TM-β-CD add to the bulkiness of the host and, most likely, have an effect on complex destabilization.

Also, the orientation of the 2-AN molecule inside the CD cavity is better understood. Since the sixth position -OH group has little to do with complex stabilization, it is likely that the 2-AN fits lengthwise into the cavity, with the acetyl group emerging from the wide rim of the CD,[7] Figure 14.

Figure 14. Proposed 2-AN:β-CD inclusion complex.

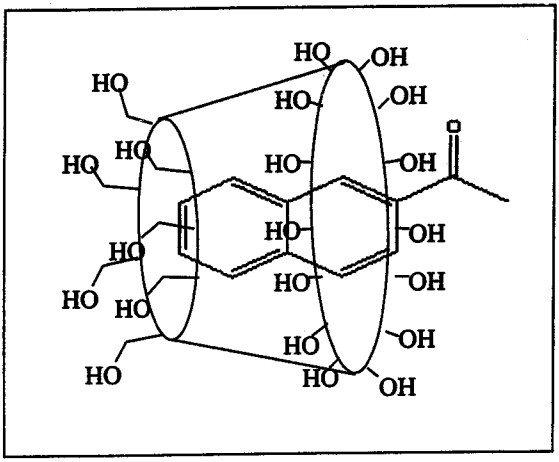
HO
OH
HO
OH
HO
HO
HO
OH
HO
OH
HO
HO
HO
OH
HO
HO
HO
OH
HO
OH
HO
OH

II. 1,5-DNSA with TM-β-CD.

Fluorescence binding constant studies of the 1,5-DNSA:β-CD complex were initially performed by Catena and Bright.[7] The published binding constants are 100 M^{-1} at 15 °C and 60 M^{-1} at 25 °C. The complex formation was also a topic of discussion in the thesis work of George Kosturko.[12] In order to better understand the stabilization of the 1,5-DNSA:β-CD complex, Kosturko repeated the fluorescence enhancement experiments with the use of DM-β-CD and TM-β-CD as host molecules. If sterics play a significant role in stabilization and binding interaction, K would decrease with an increase of rim -OCH_3 groups, which hinder complexation. That is, K would decrease from β-CD to DM-β-CD to TM-β-CD. Kosturko's results, however, showed the opposite trend. The reported results for binding constants are 917 ± 154 M^{-1} and $2.0 \pm 0.6 \times 10^3$ M^{-1} for DM-β-CD and TM-β-CD, respectively.[12] The extremely high binding constants are unusual and certainly a source for further investigation.

Fluorescence binding constant studies were repeated for the 1,5-DNSA:β-CD complex, and a K value of 151 M^{-1} at 22 °C was obtained. K is higher than the published values by Catena and Bright (60 M^{-1} at 25 °C, 100 M^{-1} at 15 °C),[7] and may be an effect of the temperature difference. The 1,5-DNSA:TM-β-CD binding constant measurement was also repeated and resulted in a value of 105 M^{-1}, which is more than ten times smaller than Kosturko's result. The experimental data also follow the usual steric trend, with K for TM-β-CD less than K for β-CD. This decrease in K for the TM-β-CD complex is most likely due to steric effects since the $(CH_3)_2N^-$ group of 1,5-DNSA does not participate in hydrogen bonding. Furthermore, the relatively small binding constants for the 1,5-DNSA complexes are most likely due to the expanded width of the molecule

upon substitution. The more common equatorial approach is disfavored since the wide guest molecule does not fit easily into the cyclodextrin cavity.[7] Fewer and less stable complexes form and a small K value results.

III. 2,6-MANS with TM-β-CD.

Catena and Bright also studied the complex formation of 2,6-MANS with β-CD. The researchers found both 1:1 and 2:1 β-CD:2,6-MANS complexation with binding constants of 7360 M^{-1} and 300 M^{-1} at 25 °C, respectively.[7] The study attributes the stabilization of the 1:1 complex to hydrogen bonding between the sixth position -OH group at the tapered rim of the β-CD and the deprotonated sulfonate group of 2,6-MANS. The 2:1 complex, however, is stabilized by the cyclodextrin's protection of the methyl and benzene groups of 2,6-MANS from the aqueous solvent, known as the hydrophobic effect. Also, Werner et. al. suggest that the -OH groups at each CD's wide rim, may interact through hydrogen bonding and further stabilize β-CD complexes.[10]

The fluorescence binding constant studies with 2,6-MANS were repeated using TM-β-CD as the host molecule. The binding constants of the system are found in Table 13 and were determined using a linear double-reciprocal equation (Eq. 7), and a non-linear least squares equation (Eq. 8) fit with both Mathematica and Excel,[13] which each used the linear results as initial guesses.

$$1/\Delta F = 1/([CD]K\Delta F + 1/\Delta F_\infty \qquad (7)$$

$$\Delta F = (\Delta F_\infty K [CD]) / 1 + K [CD] \qquad (8)$$

The non-linear regression methods give more accurate binding constants than the linear method since the lower the CD concentration, the larger the reciprocal of Eq. 7, and the greater the error in measurement.

Each of non-linear regression methods resulted in a K value of ~4800 M^{-1} at 25 °C for the 2,6-MANS:TM-β-CD complex (Table 13). It appeared that only one inclusion complex, 1:1, was observed using the fully methylated β-CD. Catena and Bright, however, showed evidence for 1:1 and 2:1 β-CD:2,6-MANS complexes at β-CD concentrations below 0.010 M. In order to see any evidence for a 2:1 complex formation between TM-β-CD and 2,6-MANS, additional fluorescence enhancement studies were performed with more highly concentrated cyclodextrin sample solutions. The results are included in Figure 11 and show the overlap of 0.01-0.02 M TM-β-CD sample spectra. There is clearly no evidence for a 2:1 complex with TM-β-CD and 2,6-MANS.

The absence of a 2:1 TM-β-CD:2-AN complex is further supported by Ealing space filling models. Since the TM-β-CD has a more extended, or deeper, cavity than β-CD, the 2,6-MANS guest slips further into the hydrophobic cavity and only a small portion of the molecule is exposed. The second TM-β-CD is, therefore, less likely to complex in order to protect such a small region of the molecule. Also, unlike β-CD, TM-β-CD has no opportunity for hydrogen bonding between the cyclodextrins' wide rim -OH groups. There exists little driving force for the formation of a 2:1 TM-β-CD:2,6-MANS complex.

The 1:1 complex formation between 2,6-MANS and TM-β-CD is also an area of interest. Unlike the relatively low binding constants observed for 1,5-DNSA, the K values for 2,6-MANS are ~4800 M^{-1} for TM-β-CD and 7360 M^{-1} for β-CD. Since the

substitution of the 2,6-MANS molecule affects the length and not the width of the fluorophore, the binding constants are much higher than those for 1,5-DNSA.

A binding constant of ~4800 M^{-1} for 2,6-MANS binding to TM-β-CD is significantly less than the published K of 7360 M^{-1} for binding to β-CD at a similar temperature. Catena and Bright attributed the 1:1 complex of 2,6-MANS:β-CD to hydrogen bonding between the guest SO_3^- group and the -OH groups at the tapered rim of the CD.[7] The binding constant, however, is still significantly high for TM-β-CD, which does not have any hydrogen bonding capabilities for SO_3^-. If hydrogen bonding were solely responsible for the strong 2,6-MANS:β-CD complex, K would not be as great for the TM-β-CD experiments. Other factors, such as the more hydrophobic cavity of the methylated CD, must account for the high binding constant.

The greater binding constant observed for the 2,6-MANS:β-CD complex compared to the TM-β-CD complex can be investigated using thermodynamic data. According to Catena and Bright, the 2,6-MANS:β-CD complex is both enthalpically and entropically favored. An enthalpy value of -6.7 kJ/mol is attributed to the hydrophobic interaction of 2,6-MANS with the β-CD walls. The entropy was reported as 51.8 J/Kmol and is a consequence of the 2,6-MANS entering the β-CD cavity.[7] The guest replaces the polar water molecules and disrupts the low entropy solvent shell surrounding 2,6-MANS. Thermodynamic studies of 2,6-MANS binding with TM-β-CD, however, resulted in more negative enthalpy and entropy values. The enthalpy of the 2,6-MANS:TM-β-CD complex was calculated as -35 ± 3 kJ/mol. The methyl groups of the TM-β-CD make the cavity environment more hydrophobic than the natural β-CD cavity, creating much stronger guest:host interactions.

A different result was obtained for the entropy parameter. An average ΔS value of -47 ± 8 J/Kmol was calculated for the TM-β-CD complex, a much less favorable value than the 50 J/Kmol published for the β-CD complex. The methyl groups of the TM-β-CD restrict the motion of 2,6-MANS, which overcomes the favored entropic effects of solvent replacement and solvent shell disturbance. Although the TM-β-CD complex is more enthalpically stable than the β-CD complex, the less favorable entropy term dominates the thermodynamic parameters and a lower binding constant is observed.

IV. 2,6-TNS with TM-β-CD.

Catena and Bright also performed fluorescence enhancement studies with 2,6-TNS and β-CD.[7] 2,6-TNS differs from 2,6-MANS in the position of the methyl substituent (Figure 2). The methyl group of 2,6-MANS is bonded to the nitrogen atom, between the phenyl and naphthalene portions of the molecule. The methyl group of 2,6-TNS, however, is positioned on the phenyl ring in a para orientation from the anilino nitrogen. Similar to 2,6-MANS, however, both 1:1 and 2:1 complexes were detected with binding constants of 1980 M^{-1} and 600 M^{-1}, respectively.[7] Catena and Bright attribute the formation of both complexes to the same effects discussed for 2,6-MANS. The 1:1 complex is stabilized by hydrogen bonding between the guest SO_3^- group and the -OH groups at the sixth position of the CD, while the 2:1 complex is formed due to the hydrophobic effect and the protection of the methyl and benzene portions of the guest molecule.[7]

A binding constant of 22358 M^{-1} was measured for the 1:1 complex formation of 2,6-TNS with TM-β-CD. Similar to the 2,6-MANS results, there was no evidence for the

2:1 complex formation with TM-β-CD. The 2,6-TNS molecule may slip deeper into the TM-β-CD cavity, burying the anilino nitrogen and the phenyl ring, at least partially. As a result, the phenyl ring is not exposed enough to form a 2:1 complex.

Unlike the previous study with 2,6-MANS, the binding constant of the 2,6-TNS 1:1 complex is greater with the TM-β-CD (2358 M^{-1}) than it is with β-CD (1980 M^{-1}),[7] although not by much. The more hydrophobic cavity of the TM-β-CD must compensate for the loss of hydrogen bonding between the guest SO_3^- group and the -OH groups on the narrow rim of β-CD. In order to make any further conclusions, the experiment must be repeated and thermodynamic data should be obtained.

REFERENCES

1a. J. Szetli, *Cyclodextrin Inclusion Complexes*. Akademiai Kiado, Budapest, 1982.
b. http//www.natur.cuni.cz/~jindrich/CD/. Jindrich Jindrich, Department of Chemistry; Charles University; Prague, Czech Republic.

2. K. Shimada, Y. Kurata, T. Oe. *J. Liquid Chromatogr.* **1990**, 13, 493.

3. Cline-Love, L. J., Grayeski, M.L., Noroski, J., Weinberger, R. *Anal. Chim. Acta.* **1985**, 170, 3.

4. W.G. Herkstroeter, P.A. Martic, S. Farid. *J. Amer. Chem. Soc.* **1990**, 112, 3583.

5. G. Weber, H.G. Dreckamer, P.M. Torgerson. *Biochem.* **1979**, 18, 3079.

6. Rajewski RA, Stella VJ. *J Pharm Sci.***1996**, 11, 1142-69.

7. Catena, G.C., Bright, F.V. *Anal. Chem.* **1989**, 61, 915.

8. Fraiji, E.K., Cregan, T.R., Werner, T.C. *Appl. Spectr.* **1994**, 48, 79.

9. Madrid, J.M., Mendicuti, F. *Appl. Spect.* **1997**, 51, 1621.

10. Werner, T.C., LaRose, J., Anderson, J.S. *Proceedings of the Ninth International Symposium on Cyclodextrins*. **1999**, 67.

11. J. Szejtli. *Cylcodextrin Technology*; Kluwer: Dordrecht, 1988.

12. Kosturko, G. *The Use of Fluorescence Properties of Substituted Naphthalenes and Pyrene to Study Their Binding to β-Cyclodextrins*. Union College Senior Thesis, 2002.

13. Scientific Data Analysis Software, A. M. Halpern, S. L. Frye and M. Huber. Prentice Hall, 2003.

Part II.
The Use of Capillary Electrophoresis with Cyclodextrin Additives for the Separation of LSD, LAMPA, and iso-LSD.

INTRODUCTION

The desire to electrophoretically separate lysergic acid diethylamide (LSD) from other similarly structured molecules originated at the Drug Chemistry department of the NYS Forensic Investigation Center. When an assumed LSD sample is brought to the lab, it is usually in the form of a powder, liquid, or blotter paper. The chemists then perform a series of procedures in order to legally prove that the LSD is indeed controlled LSD and not another molecule called LAMPA, which is not a controlled substance. LSD and lysergic acid methyl propyl amide (LAMPA) have the same molecular weight and differ only in the carbon linkage off of the amide portion of the molecule, Figure 1. LSD has two ethyl groups, while LAMPA has both a methyl and a propyl group.

Currently, the Forensic Center's analysis of an LSD sample includes three different steps.[1] An Ehrlich color test is first employed to look for a violet color produced by an LSD-like molecule. If a violet color is detected, Thin Layer Chromatography is used with LSD and LAMPA standards to separate and identify the LSD. Finally, Gas Chromatography with Mass Spectrometry detection and/or Fourier Transfer Infrared Spectroscopy is performed to confirm structure. These combined procedures are time consuming. Capillary Electrophoresis (CE) in combination with the Ehrlich color test may allow an efficient separation and identification of LSD in a simpler way. CE achieves high resolution in a short period of time with a very small sample volume. Little sample preparation is required and reagents are not expensive. CE separates analytes with similar structures, and a UV/Visible detector can provide absorbance data at either a specific wavelength or a complete spectrum.

Figure 1. Structures of LSD and LAMPA.

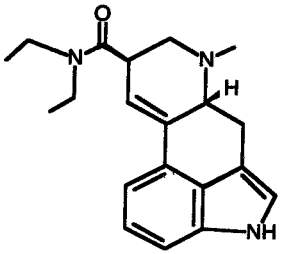

LSD

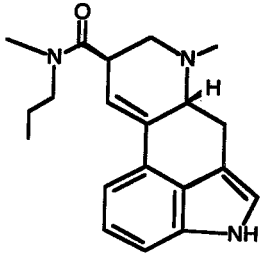

LAMPA

The instrumentation used includes a buffer-filled silica capillary with each end immersed in identical buffer solutions. A high voltage is applied to create charge at each electrode. The sample is normally injected at the positive anode, and the electric field carries the analytes through the capillary and toward the negative end. The analytes eventually reach the detector at a time depending on their individual mobilities.

There are two different effects that combine to establish an analyte's overall mobility. The first is the electrophoretic mobility, Figure 2. The electrophoretic mobility is a constant of proportionality between the velocity of the analyte as it moves through the capillary and the strength of the electric field.[2] When an ion in solution is placed in an electric field, the charge of the analyte, as well as a retarding frictional force, have an effect on the velocity. The mobility is, therefore, proportional to the charge of the ion and inversely proportional to the frictional coefficient, Eq. 1.[2]

$$\mu_{ep} = q/f \qquad (1)$$

The effect of frictional force is characterized by Stoke's Law in Eq. 2.[2]

$$f = 6\pi\eta r, \qquad (2)$$

where f is the frictional coefficient, η is the viscosity of the solution, and r is the analyte's ionic radius. Thus, the size of the analyte, as represented by the ionic radius, also modifies the electrophoretic mobility. The greater the radius, or larger the molecule, the greater the frictional drag and the smaller the mobility. Ultimately, as the analytes flow toward the negative cathode, they are separated based on their size and charge. Smaller, more positively charged molecules, for example, move more rapidly toward the negative end of the capillary than less positively charged ions, or as larger ions with the same positive charge. Negatively charged ions actually

travel in the opposite direction. Neutral analytes, which fall between the two, exhibit no charge and no electrophoretic flow.

Electroosmotic flow (EOF) is the other mobility determining factor, Figure 3. Because the silica capillary is negatively charged, the positive cations of the buffer are attracted to the walls. Some of the cations are tightly held at the walls, while others form a double-layer beside them. This double-layer, with an excess positive charge, has a net movement toward the negative charge at the cathode and acts as a pump to carry the analytes along with it.

The EOF is affected by many experimental variables, including buffer concentration, buffer pH, temperature, viscosity, field strength, surfactants, and buffer additives. As defined by Smoluchowski,[3] the electroosmotic velocity is expressed as,

$$v_{eo} = E \cdot \varepsilon\zeta / \eta, \qquad (3)$$

where ε is the dielectric constant, η is the viscosity of the buffer, and ζ is the zeta potential of the liquid-solid interface, resulting from the negative charge on the capillary wall. As the viscosity of the buffer solution is increased, it is more difficult for the analytes to flow through the capillary and the electroosmotic flow is not as great.

The overall mobility of capillary electrophoresis is equal to the sum of the electrophoretic and electroosmotic mobilities.

$$\mu = \mu_{ep} + \mu_{eo} \qquad (4)^3$$

Also, the velocity of a given analyte is equal to the product of its mobility with the constant electric field strength. It is also inversely proportional to the capillary length.

$$v = \mu E = \mu V/L, \qquad (5)^4$$

where V is the voltage and L is the capillary length.

Figure 2. Electrophoretic flow.

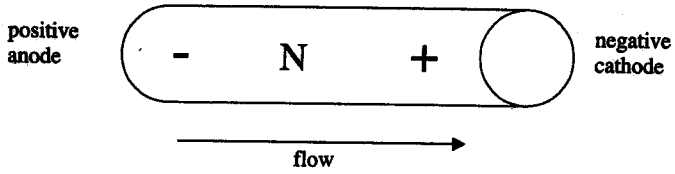
positive
anode
-
N
+
negative
cathode
flow

Figure 3. Electroosmotic flow.

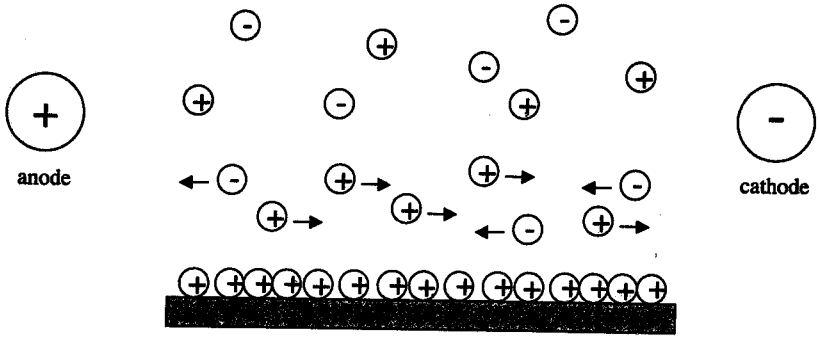
anode
cathode

In a CE run, positively charged analytes elude first as they are most strongly attracted to the other end of the capillary. Neutral analytes follow, since they do not exhibit any electrophoretic flow. Negatively charged analytes elude last, with an electrophoretic flow in the opposite direction of the similarly charged cathode. Size is also a factor. Small, positive molecules, for example, move more rapidly through the capillary than larger molecules with the same positive charge. Small, negatively charged analytes, on the other hand, follow the larger molecules of the same negative charge.

As buffer additives, cyclodextrins (CDs) can interact with the analytes and achieve separation. These large, bucket shaped molecules are made up of glucose subunits. α, β, and γ CDs have 6,7,and 8 glucose units, respectively, Figure 4.[5] In a dynamic system, the analytes of a sample bind in the hydrophobic cavity of the CD. The -OH groups at the second, third and sixth positions of each glucose unit may be substituted by a variety of substituents; methyl and sulfate groups are common examples. The size and charge of the substituents determine the extent of interaction the analyte will have with the CD. Cyclodextrins are also advantageous in their ability to separate chiral molecules.

Along with LSD and LAMPA, there are other LSD-like molecules that may appear in a forensic evidence investigation. Iso-LSD is a diastereomer of LSD, but it is not a controlled substance, Figure 5. The molecule is often found in the analyses of LSD samples and, if distinguishable by CE, it would be advantageous to use a separation method that included all three analytes. Furthermore, nor-LSD and nor-iso-LSD are analytes of interest, Figure 5. These molecules are metabolites of LSD and may be useful in the analysis of toxicology samples, primarily blood and urine.

Figure 4. Structure of the natural cyclodextrin.

a. side view, b. top view.

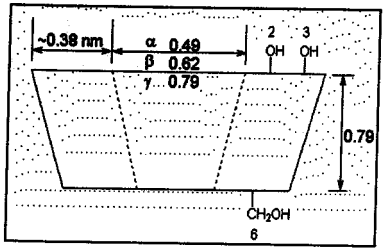
~0.38 nm
α 0.49
β 0.62
γ 0.79
2
3
OH
OH
0.79
CH2OH
6

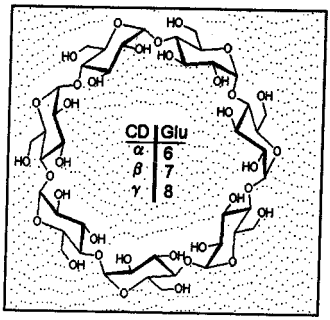
CD | Glu
α | 6
β | 7
γ | 8

Figure 5. Structures of iso-LSD, nor-LSD and nor-iso-LSD.

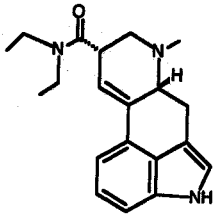

iso-LSD

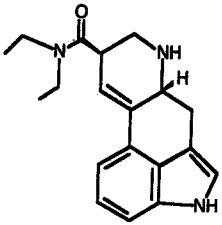

nor-LSD

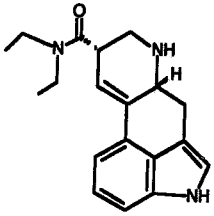

nor-iso-LSD

EXPERIMENTAL

The LSD (1mg/mL), iso-LSD (1mg/mL), nor-LSD with nor-iso-LSD (100μg/mL), and LAMPA (1mg/mL) stock solutions (dissolved in acetonitrile) were received from Cerilliant. The stocks were each transferred from ampules into amber vials with sealed caps for freezer storage. γ-cyclodextrin and dimethyl-β-cyclodextrin (two -OH groups converted to $-OCH_3$) were received from Cerestar, trimethyl-β-cyclodextrin (three -OH groups converted to $-OCH_3$) from Aldrich, and α-cyclodextrin from Wacker. The sulfated-β-cyclodextrin was first received from American Maize-Products Company (with approximately 14 $-SO_3^-$ groups per β-CD), and then reordered from Aldrich (with approximately 9 $-SO_3^-$ groups per β-CD), along with the sulfated-α-cyclodextrin (with an assumed 50% sulfated and approximately 9 $-SO_3^-$ groups per α-cyclodextrin). The α-CD Polymer, with glyceryl linkages, was obtained from Cyclolab. The general formula of the polymers is as shown below:

$$[\alpha\text{CD-}(CH_2\text{-}CHOH\text{-}CH_2\text{-}O)_n X]_p$$

where X is H or CD; p is >1 but <6-8; and n is >1 but <18.[6] Cyclolab reports the average % CD as 54.[6]

Sample solutions were prepared by adding 75μL of the stock solution(s) to 0.70 mL millipore water and 0.30 mL acetonitrile. The components were allowed to mix thoroughly before being filtered (with B-D Latex Free Syringes) into sealed plastic vials.

Sample runs with buffer solution only did not separate LSD and LAMPA. Cyclodextrins were then added to the buffer in an attempt to resolve the analytes. The cyclodextrin additives were weighed and dissolved in the appropriate volume of acetate, borate, or citrate buffer solution of a particular pH.

Unless otherwise specified, the experimental conditions of each CE run remained unchanged. The temperature was set at 25°C and a 20kV voltage was applied across the capillary. A 5.00 minute flush with the desired buffer preceded the injection, which was accomplished by applying 50.0 mbar pressure for 4.00 seconds. Absorbance data were collected at 214, 240, and 320 nm with a threshold of 1.00 mAU.

RESULTS

Part A: Separation at low pH.

I. Separation of samples containing LSD and LAMPA.

A. TM-β-CD, DM-β-CD, and γ-CD.

Each of the three CDs were used in 50 mM acetate buffer, pH 4.03. No separation was observed using TM-β-CD at 40 and 60 mM and DM-β-CD at 60 mM. Partial separation was observed using γ-CD (R = 0.29). Migration times were in the range of 9-11 minutes; which is longer than without the presence of any CDs (~6 min.).

B. α-CD.

Table 1 below summarizes the results using α-CD with an LSD + LAMPA sample mixture.

Trial #	[CD] (mM)	Acetate Buffer, pH 4.03 (mM)	Temp (°C)	t_m (min)	R	File	Date; Notebook
1	60	50	25	9.45, 10.02	2.55	007-0301...3	6/26/02; 005(Y)
2	60	50	25	9.99, 10.64	2.79	LSDLMPA13-15	6/27/02; 006
3	60	50	25	10.09, 10.75	2.86	LSDLMPA16-18	6/27/02; 006
4	60	50	25	7.34, 7.66	2.39	BUFTES15	7/9/02; 009
5	60	50	25	7.65, 7.99		BUFTES16-18	7/10/02; 009(Y)
6*	60	50	25	7.80, 8.20	2.65	BUFTES88-90	7/22/02; 013-013(Y)
7*	60	50	25	7.59, 7.96	2.47	BUFTES91-93	7/23/02; 013(Y)
8*	60	50	25	7.58, 7.95	2.49	BUFTES94-96	7/23/02; 013(Y)
9*	60	50	25	7.92, 8.32	2.48	BUFTES97-99	7/24/02; 013(Y)
10*	60	50	25	7.88, 8.28	2.49	BUFTE100-102	7/24/02; 013(Y)
11*	60	50	25	7.96, 8.36	2.51	BUFTE103-105	7/24/02; 013(Y)
12	60	50	15	8.15, 8.49	1.97	BUFTE163-165	8/1/02; 015(Y)-016

*Trials used in reproducibility data.

Trials #6-11 in Table 1 were performed over a series of three days to observe the inter-day reproducibility characteristics of the conditions. The following data describe the averages ± standard deviations, and relative standard deviation values (in parenthesis) for the peak migration times (peak 1, peak 2) and the resolution, respectively; 7.8 ± 0.2 (3%), 8.2 ± 0.2 (2%), 2.52 ± 0.07 (3%). Trials #9-11 were used in the calculations for the following intra-day data; 7.92 ± 0.04 (0.5%), 8.32 ± 0.04 (0.5%), 2.49 ± 0.02 (0.8%).

C. α-CD + Aldrich sulfated-β-CD.

The analysis was performed with 60 mM α-CD and 0.2 mM sulfated-β-CD in 50 mM acetate buffer, pH 4.03 at 25°C. Although separation of LSD and LAMPA was achieved on the order of 8 minutes (R = 1.8), the resolution was not a great as with α-CD only. (See Table 1).

II. Separation of samples containing LSD, LAMPA, ar iso-LSD.

A. α-CD.

Table 2 below summarizes the results using α-CD with a sample mixture containing LSD, LAMPA, and iso-LSD.

Trial #	[CD] (mM)	Acetate buffer, pH 4.03 (mM)	Temp (°C)	t_m (min)	$R_{1,2}$	$R_{2,3}$	File	Date; Notebook
1	60	50	25	9.91, 10.05	0.82	2.32	LSDLMPA19-21	6/27/02; 006
2	80	50	25	8.05, 8.16, 8.47	0.82	1.17	L_LM_IL1-3	6/28/02; 006-006(Y)
3	40	50	25	6.59, 6.63, 6.87	0.31	1.44	ALPHACD1-3	7/3/02; 007(Y)
4	60	50	25	7.29, 7.38, 7.64	0.68	1.63	ALPHACD4-6	7/3/02; 007(Y)
5	80	50	25	7.76, 7.83, 8.13	0.52	1.73	ALPHACD7-9	7/3/02; 007(Y)
6	60	50	25	7.76, 7.85, 8.13	0.86	1.86	BUFTES19	7/10/02; 009(Y)
7	60	50	25	7.52, 7.6, 7.89	0.80	2.04	BUFTES23-25	7/12/02; 010
8	60	50	25	7.82, 7.88, 8.21	0.47	2.12	BUFTES26-28	7/15/02; 010
9	60	50 (Citrate)	25	16.81, 16.95, 18.67	0.55	4.13	BUFTES47-49	7/17/02; 011-011(Y)
10	60	50	25	8.37, 8.47, 8.824	0.83	2.04	BUFTE109	7/25/02; 014
11	60	50	15	12.77, 13.03, 13.41	1.62	1.48	BUFTE125-126	7/26/02; 014-014(Y)
12	60	50	15	12.20, 12.50, 12.90	1.4	1.68	BUFTE127-129	7/26/02; 014-014(Y)
13	60	50	20	10.76, 10.95, 11.39	1.15	1.92	BUFTE130-132	7/26/02; 014-014(Y)
14	60	50	15	8.21, 8.32, 8.43	1.1	1.64	BUFTE166-168	8/1/02; 015(Y)-016
15	60	50	15	8.69, 9.34, 9.48	1.1	1.65	BUFTE178-180	8/2/02; 017
16	60	50	15	9.80, 11.90 12.10	1.4	2.11	BUFTE182-183	8/2/02; 017
17*	60	50	15	8.28, 8.38, 8.66	0.97	1.50	BUFTE306-308	11/5/02; 023(Y)
18*	60	50	15	9.06, 9.18, 9.50	1.11	1.59	BUFTE312-314	11/6/02; 023(Y)
19*~	60	50	15	8.48, 8.54, 8.82	0.54	1.60	BUFTE318-323	11/7/02; 023(Y)

*Trials used in reproducibility data.
~Only three of six injections used for average migration time and resolution data.

Electropherograms of Trials #3, 4, and 5 in Table 2 are included in Figures 6, 7, and 8, respectively.
The electropherogram of Trial #15 in Table 2 is included in Figure 9.

Trials #17-19 in Table 2 were performed over a series of three days in order to observe the inter-day and intra-day reproducibility characteristics of the conditions. The following data describe the averages ± standard deviations, and relative standard deviation values (in parenthesis) for the peak migration times (peak1, peak 2, peak 3) and the resolution ($R_{1,2}$, $R_{2,3}$), respectively; 8.61 ± 0.4 (5%), 8.70 ± 0.4 (5%), 8.99 ± 0.4 (5%), 0.9 ± 0.3 (34%), 1.6 ± 0.06 (4%). Trial #19 (three of six injections) were used in the calculations for the following intra-day data; 8.48 ± 0.05 (0.5%), 8.54 ± 0.07 (0.8%), 8.82 ± 0.03 (0.3%), 0.54 ± 0.4 (66%), 1.6 ± 0.3 (18%).

Upon trial with 50 mM Citrate buffer, there was no significant improvement of the results. Migration times were longer, and $R_{2,3}$ was improved, but $R_{1,2}$ was lower than in most other trials.

Figure 6. Separation of LSD, LAMPA and iso-LSD with 40 mM α-CD, 50 mM acetate buffer, pH 4.03, 25 °C.

Current Electropherogram(s)

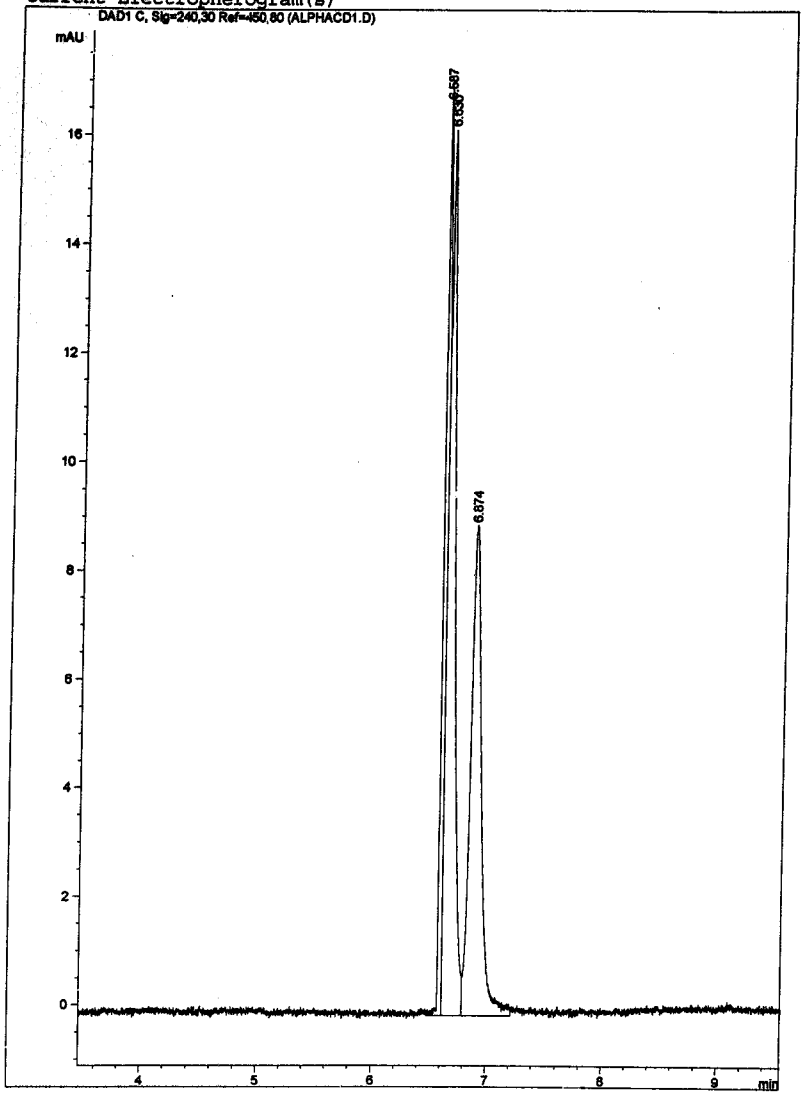

Figure 7. Separation of LSD, LAMPA and iso-LSD with 60 mM α-CD, 50 mM acetate buffer, pH 4.03, 25 °C.

Current Electropherogram(s)

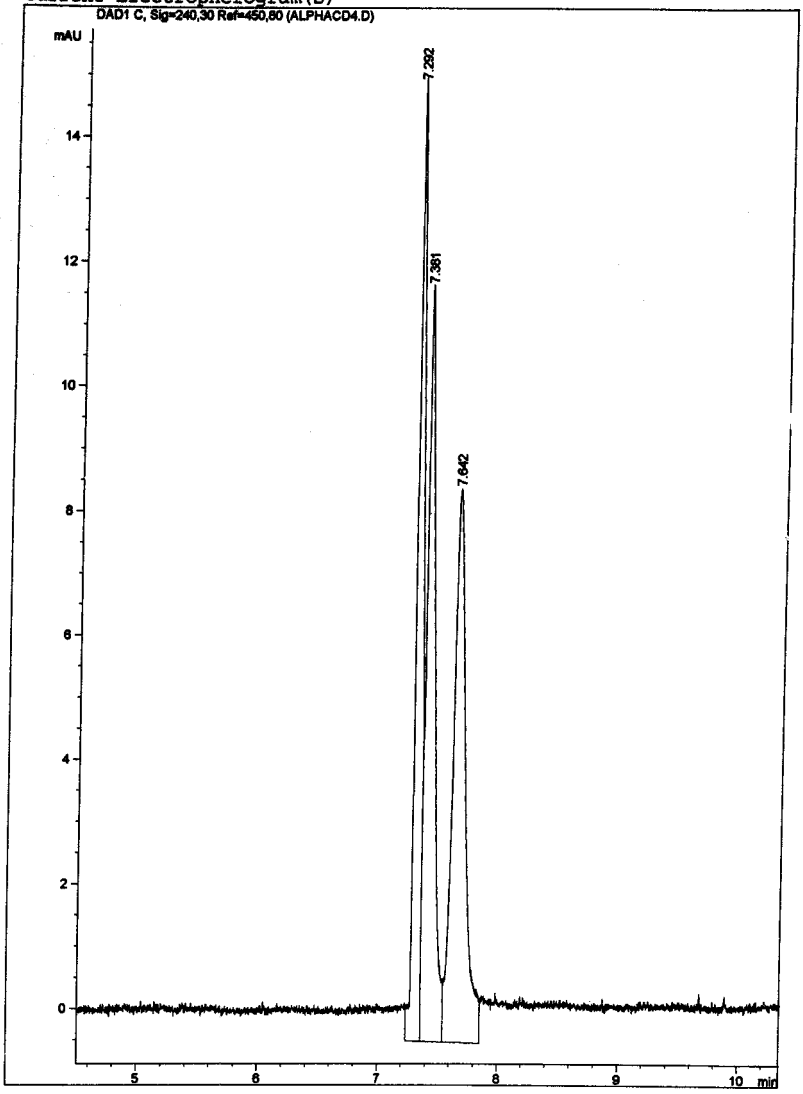

Figure 8. Separation of LSD, LAMPA and iso-LSD with 80 mM α-CD, 50 mM acetate buffer, pH 4.03, 25 °C.

Current Electropherogram(s)

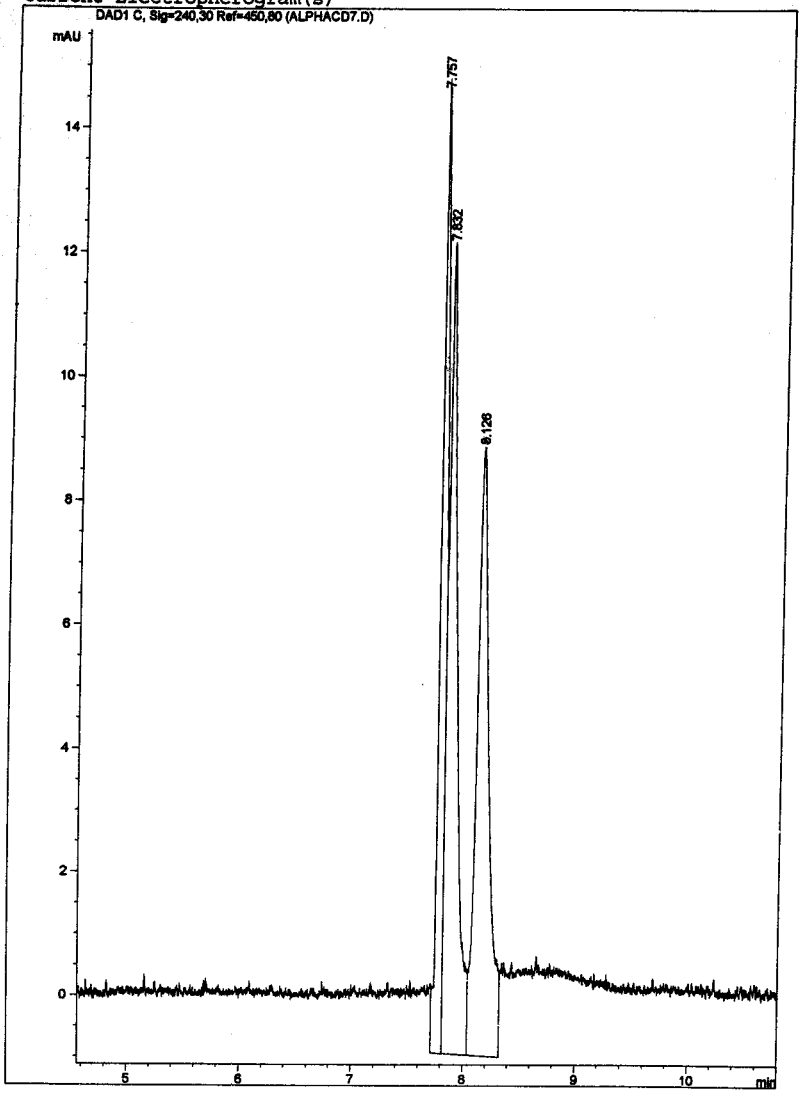

Figure 9. Separation of LSD, LAMPA and iso-LSD with 60 mM α-CD, 50 mM acetate buffer, pH 4.03, 15 °C.

Current Electropherogram(s)

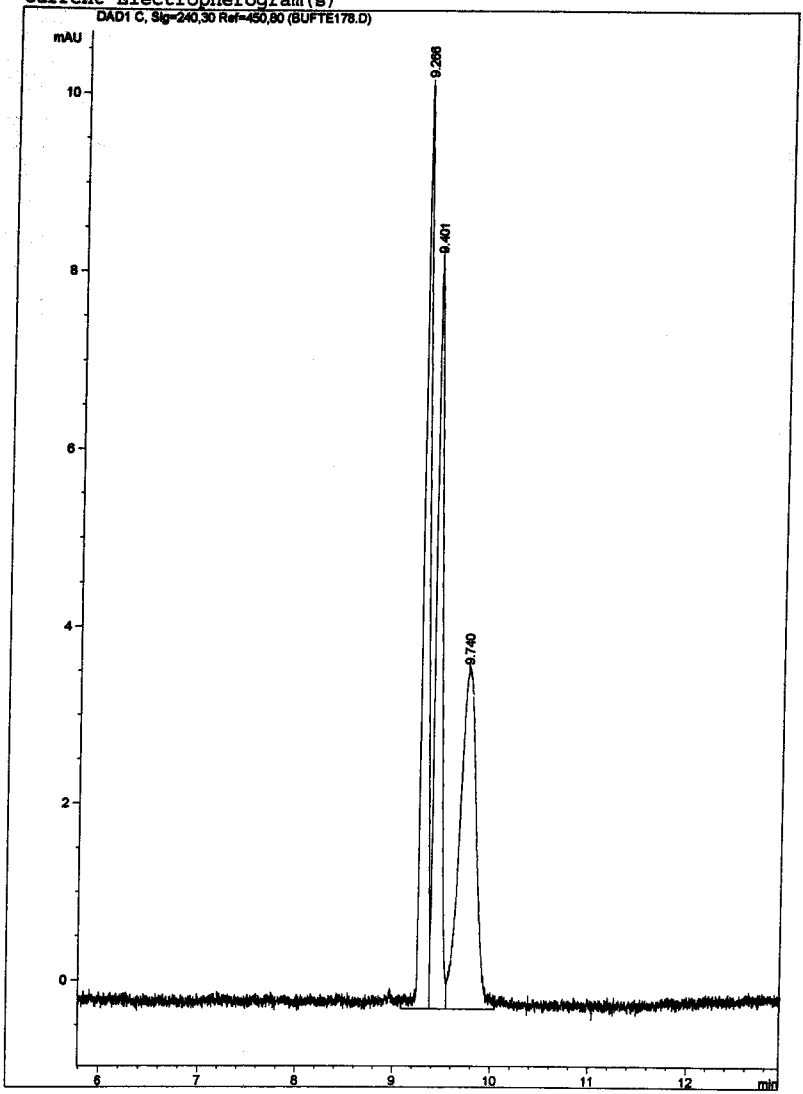

B. α-CD + (American-Maize) sulfated-β-CD.

Table 3 below summarizes the results using a combination of α-CD and sulfated-β-CD with an LSD, LAMPA, and iso-LSD sample mixture.

Trial #	[α-CD]/[s-β-CD] (mM)	Acetate buffer, pH 4.03 (mM)	Temp (°C)	t_m (min)	$R_{1,2}$	$R_{2,3}$	File	Date; Notebook
1	40/1	50	25				L_LM_IL4-6	7/1/02; 006(Y)-007
2	60/1	50	25	10.40, 12.05, 12.37	7.23	1.28	A_SULFB1-3	7/3/02; 007(Y)
3	60/1	25	25	10.12, 11.24, 11.76	6.93	2.23	BUFTEST1-3	7/8/02; 008-009
4	60/1	50	25	10.83, 12.30, 12.61	11.4	1.73	BUFTEST4-6	7/8/02; 008-009
5	60/1	75	25	10.60, 11.65	6.30		BUFTEST7-9	7/8/02; 008-009
6	60/1	25	25	9.73, 9.87	1.99		BUFTES10-12	7/8/02; 008-009
7	60/1	25	25	7.34, 7.66	2.39		BUFTES13-15	7/9/02; 009-009(Y)
8	60/1	50	25	10.93, 12.17, 12.21	15.5	0.71	BUFTES22	7/10/01; 009(Y)
9	60/0.1	50	25	8.20, 8.30, 8.70	0.97	2.47	BUFTES29-31	7/15/02; 010-010(Y)
10	60/0.5	50	25	10.46, 11.51	10.2		BUFTES32-34	7/15/02; 010-010(Y)
11	60/0.1	50	25	8.73, 8.83, 9.20	0.89	2.4	BUFTES35-37	7/16/02; 010(Y)-011
12	60/1	50	25	13.82, 15.71	15.9		BUFTES38-40	7/16/02; 010(Y)-011
13	60/0.1	50	25	12.20, 12.50, 13.10	1.72	2.99	BUFTES50-52	7/18/02; 012
14	60/0.2	50	25	12.40, 12.90, 13.50	3.15	2.7	BUFTESS53-55	7/18/02; 012
15	60/0.3	50	25				BUFTES56-58	7/18/02; 012
16	60/0.3	50	25	14.34, 15.69, 16.03	10.4	2.13	BUFTES68-70	7/19/02; 012(Y)
17	60/0.2	50	25	7.87, 8.17, 8.33	4.2	1.9	BUFTE175-177	8/1/02; 016-016(Y)

The electropherogram of Trial #14 in Table 3 is included as Figure 10.
Electropherograms of Trials #3, 4, and 5 in Table 3 are included as Figures 11, 12, and 13, respectively.

Figure 10. Separation of LSD, LAMPA and iso-LSD with 60 mM α-CD + 0.2 mM sulfated-β-CD, 50 mM acetate buffer, pH 4.03, 25 °C.

Current Electropherogram(s)

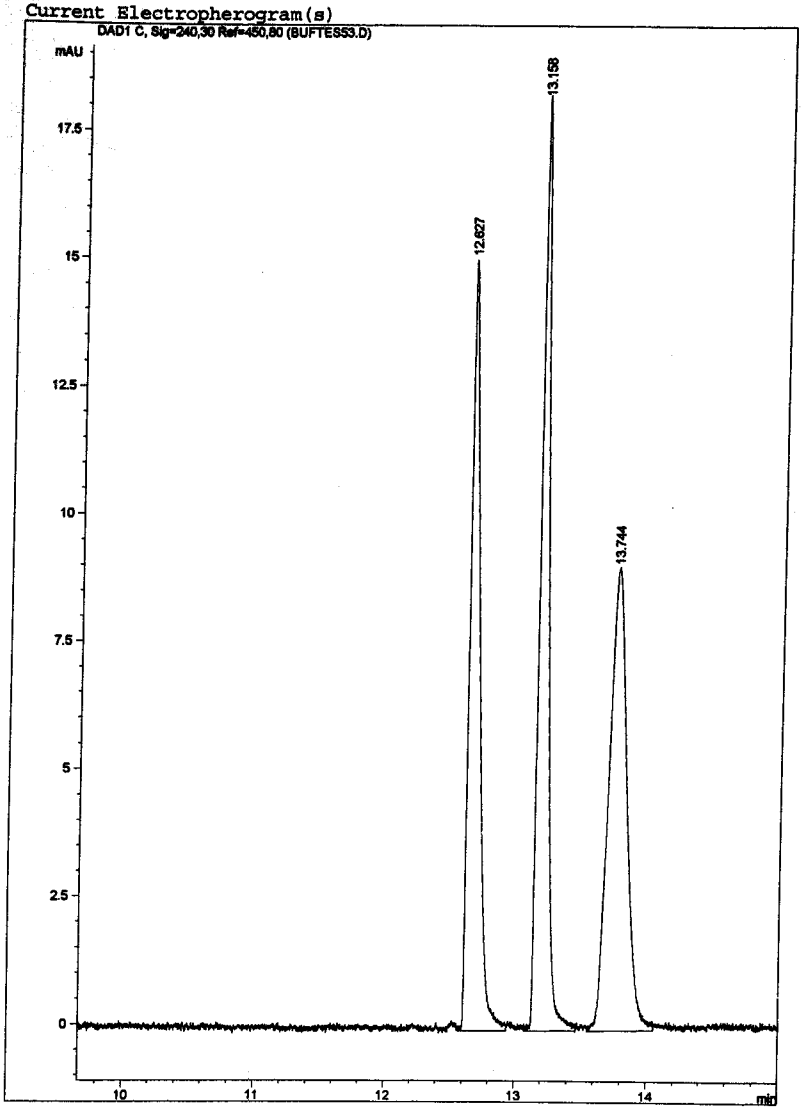

Figure 11. Separation of LSD, LAMPA and iso-LSD with 60 mM α-CD + 1.0 mM sulfated-β-CD, 25 mM acetate buffer, pH 4.03, 25 °C.

Current Electropherogram(s)

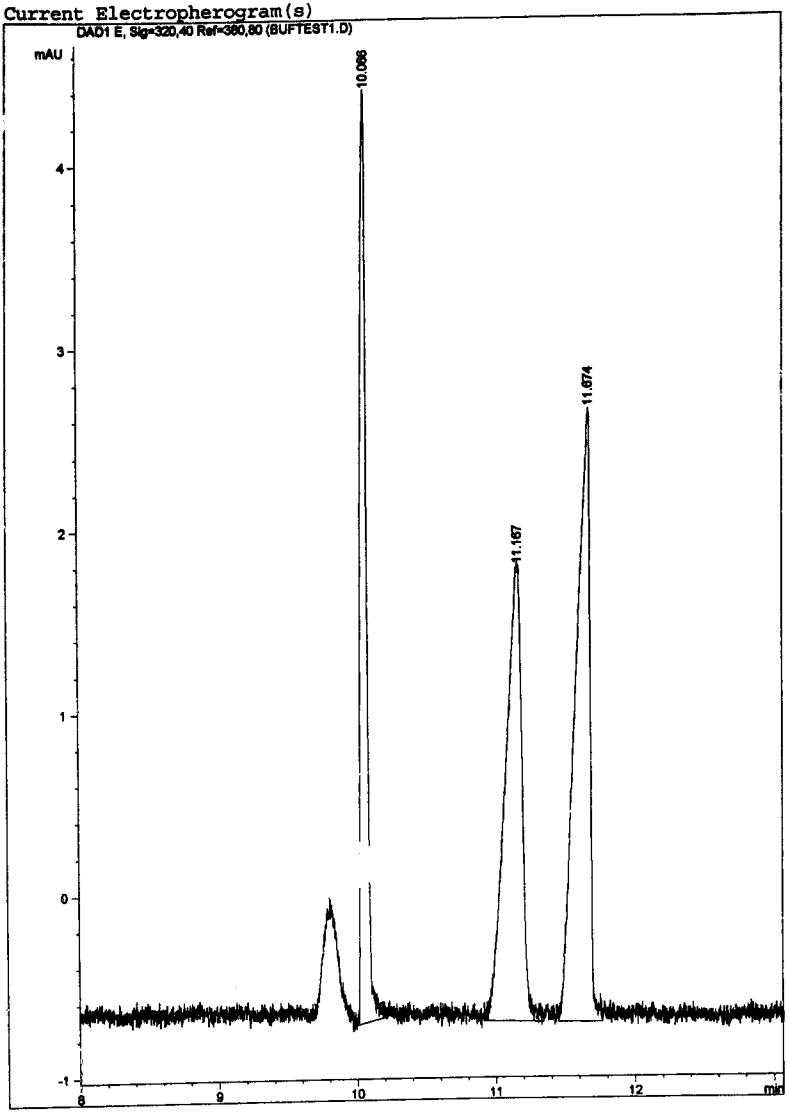

Figure 12. Separation of LSD, LAMPA and iso-LSD with 60 mM α-CD + 1.0 mM sulfated-β-CD, 50 mM acetate buffer, pH 4.03, 25 °C.

Current Electropherogram(s)

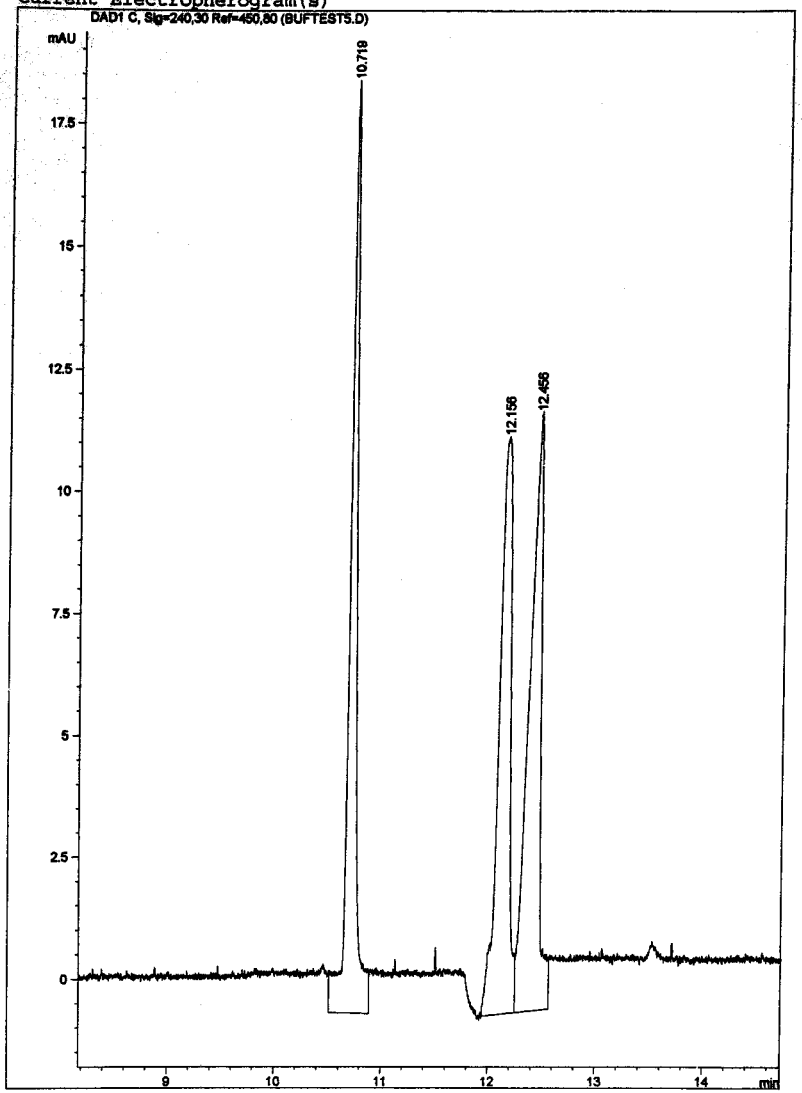

Figure 13. Separation of LSD, LAMPA and iso-LSD with 60 mM α-CD + 1.0 mM sulfated-β-CD, 75 mM acetate buffer, pH 4.03, 25 °C.

Current Electropherogram(s)

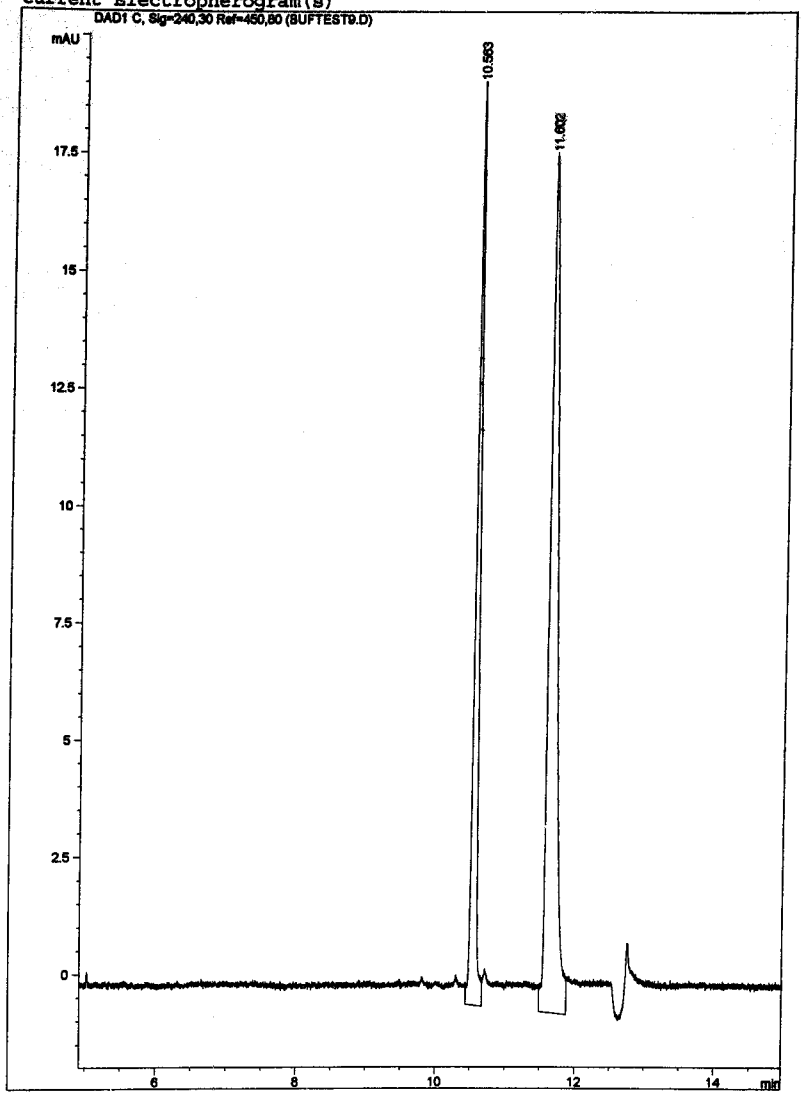

C. α-CD + (Aldrich) sulfated-β-CD.

Table 4 below summarizes the results using a combination of α-CD and sulfated-β-CD with a sample mixture consisting of LSD, LAMPA, and iso-LSD.

Trial #	[α-CD]/[s-β-CD] (mM)	Acetate buffer, pH 4.03 (mM)	Temp (°C)	t_m (min)	$R_{1,2}$	$R_{2,3}$	File	Date; Notebook
1	60/0.253	50	25	9.62, 10.49	1.83		BUFTE106-108	7/24/02; 013(Y)-014
2	60/0.129	50	25	9.97, 10.77, 10.86	8.97	1.06	BUFTE111	7/25/02; 014
3	60/0.634	50	25	12.26, 14.30, 14.53	6.52	0.42	BUFTE113	7/25/02; 014-014(Y)
4	60/0.05	50	25	9.46, 9.67, 10.05	1.97	2.66	BUFTE115	7/25/02; 014-014(Y)
5	60/0.075	50	25	9.24, 9.44	1.87	2.44	BUFTE117	7/25/02; 014-014(Y)
6	60/0.175	50	25	9.57, 9.96, 10.22	3.36	2.13	BUFTE119	7/25/02; 014-014(Y)
7	60/0.2	50	25	9.5,0 10.00, 10.02	5.4	2.04	BUFTE184-186	8/2/02; 016(Y)
8	60/0.2	50	25	9.50, 9.80, 10.20	3.0	2.9	BUFTE187-189	8/2/01; 017
9*	60/0.2	50	25	7.24, 7.49, 7.62	3.2	1.4	BUFTE309-311	11/5/02; 023(Y)
10*	60/0.2	50	25	7.84, 8.12, 8.28	3.8	1.7	BUFTE315-317	11/6/02; 023(Y)
11*	60/02	50	25	7.31, 7.55, 7.69	4.3	1.9	BUFTE324-329	11/7/02; 023(Y)

*Trials used in reproducibility data.

Trials #9-11 in Table 4 were performed over a series of three days in order to observe the inter-day and intra-day reproducibility characteristics of the conditions. The following data describe the averages ± standard deviations, and relative standard deviation values (in parenthesis) for the peak migration times (peak1, peak 2, peak 3) and the resolution ($R_{1,2}$, $R_{2,3}$), respectively; 7.46 ± 0.3 (4%), 7.72 ± 0.4 (5%), 7.86 ± 0.4 (5%), 3.8 ± 0.5 (14%), 1.7 ± 0.2 (14%). Trial #11 (six injections) were used in the calculations for the following intra-day data; 7.31 ± 0.1 (1%), 7.55 ± 0.1 (1%), 7.69 ± 0.1 (1%), 4.3 ± 0.1 (2%), 1.9 ± 0.1 (5%).

D. (American-Maize) sulfated-β-CD.

Table 5 below summarizes the results using sulfated-β-CD and a sample mixture of LSD, LAMPA, and iso-LSD.

Trial #	[CD] (mM)	Acetate buffer, pH 4.03 (mM)	Temp (°C)	t_m (min)	$R_{1,2}$	$R_{2,3}$	File	Date; Notebook
1	0.1	50	25	8.84, 9.32, 9.44	3.63	0.74	BUFTES59-61	7/18/02; 012(Y)
2	0.2	50	25	10.42, 11.40, 11.70	5.9	1.12	BUFTES62-64	7/18/02; 012(Y)
3	0.3	50	25	11.68, 13.30, 13.70	6.6	1.2	BUFTES65-67	7/18/02; 012(Y)
4	0.4	50	25	12.83, 15.06, 15.60	8.09	1.48	BUFTES71-73	7/19/02; 012(Y)
5	0.5	50	25	13.95, 16.70, 17.88	8.61	2.27	BUFTES74-76	7/19/02; 012(Y)
6	0.3	50 (Borate)	25	4.71, 4.84	2.0		BUFTES77-79	7/22/02; 012(Y)

The electropherograms of Trial #3 and 6 in Table 5 are included as Figure 14 and 15, respectively.

Figure 14. Separation of LSD, LAMPA and iso-LSD with 0.3 mM sulfated-β-CD, 50 mM acetate buffer, pH 4.03, 25 °C.

Current Electropherogram(s)

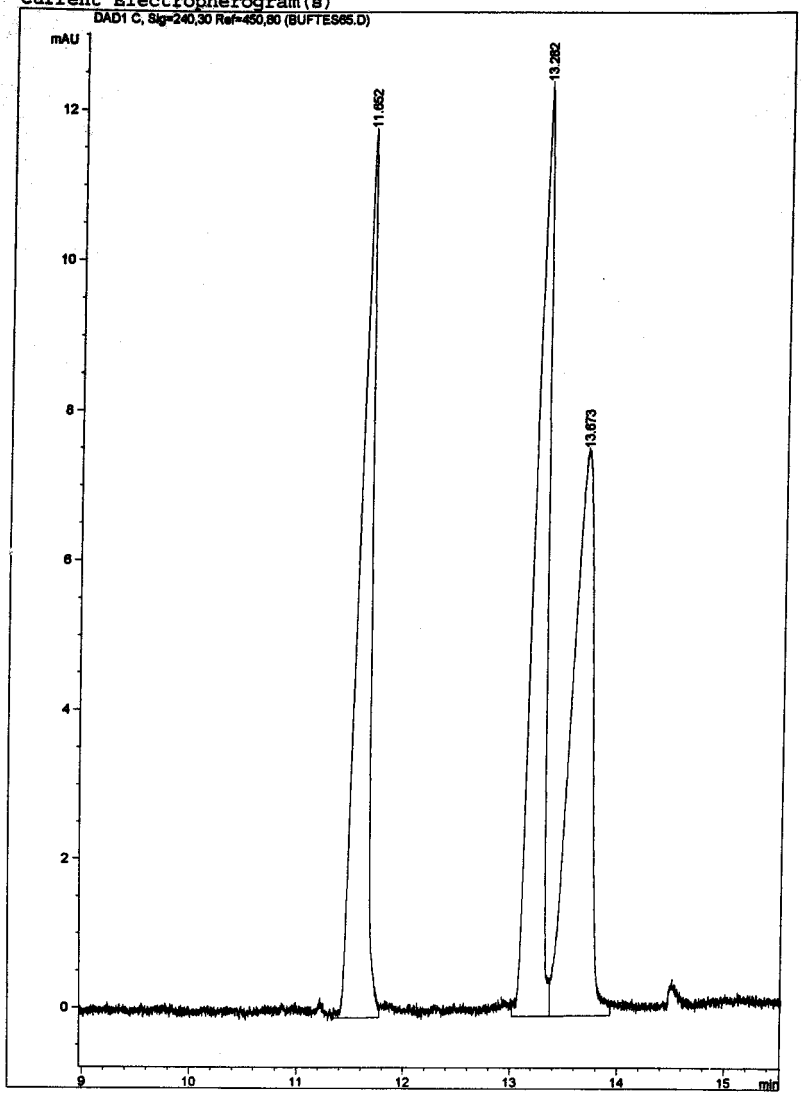

Figure 15. Separation of LSD, LAMPA and iso-LSD with 0.03 mM sulfated-β-CD, 50 mM borate buffer, pH 8.51, 25 °C.

Current Electropherogram(s)

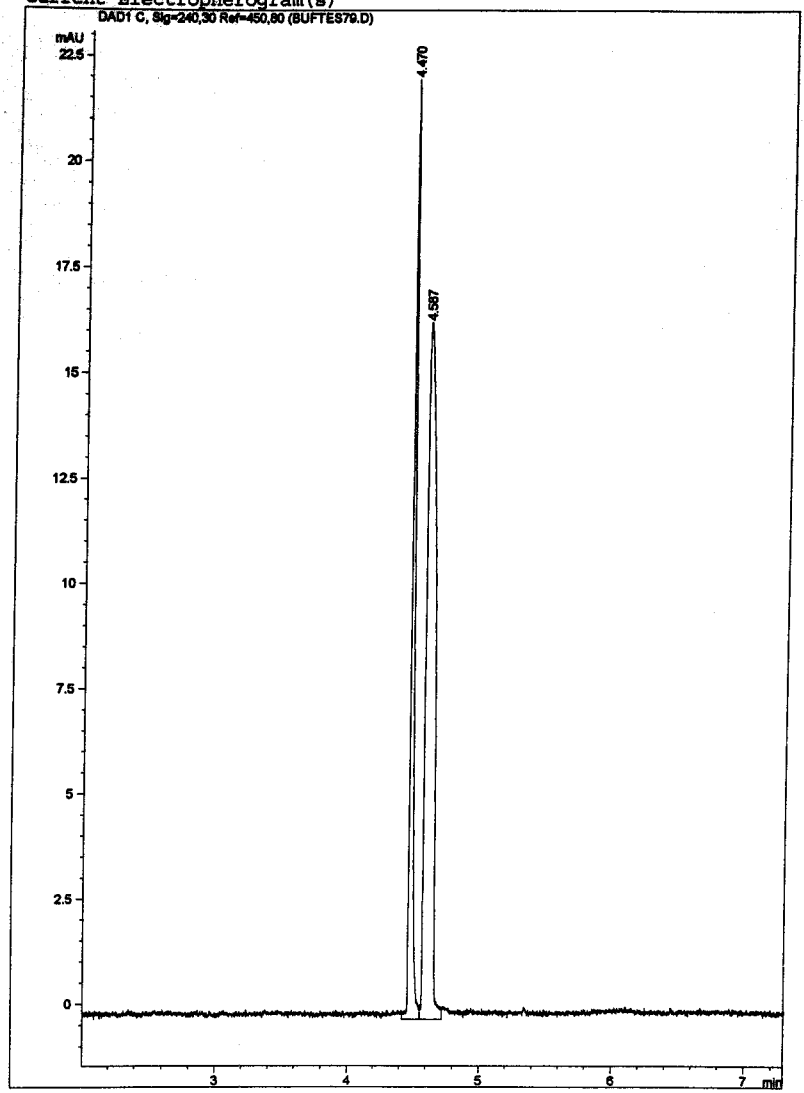

E. (Aldrich) sulfated-α-CD.
Concentrations ranging from 0.3 - 0.7 mM of sulfated-α-CD were used with 50 mM acetate buffer, pH 4.03 at 25°C. While three peaks were observed with some of the higher concentrations, there was significant overlap and the method resolution was not comparable to previous trials. The sulfated-α-CD was also used at concentrations ranging from 1- 20 mM with a 50 mM borate buffer, pH 8.51 at 25°C. Again, the three peaks were unresolved, and the peak pattern was inconsistent from run to run.

F. α-CD Polymer.
Concentrations of 10, 20, and 60 mM α-CD Polymer were used with a 50 mM acetate buffer, pH 4.03 at 25°C. The less concentrated CD trials did not resolve the three peaks, while the higher CD concentration trial resulted in no peaks within the given time window.

III. Separation of samples containing nor-LSD and nor-iso-LSD.

A. TM-β-CD, DM-β-CD, and γ-CD.
Each CD was used at a concentration of 60 mM with a 50 mM acetate buffer, pH 4.03 at 25°C. Only one peak was observed for each of the trials at about 8.5 - 9 minutes.

B. α-CD.
Again, only one peak was observed using 80 mM α-CD with a 50 mM acetate buffer, pH 4.03 at 25°C. The peak was at about 7.5 minutes.

C. α-CD + sulfated-β-CD.
A combination of 60 mM α-CD and 1 mM, as well as 0.2 mM sulfated-β-CD was used with a 50 mM acetate buffer, pH 4.03 at 25°C. Only one peak was resolved, at a migration time of about 11.5 minutes.

IV. Separation of a sample containing LSD, LAMPA, iso-LSD, nor-LSD and nor-iso-LSD.

A. α-CD + sulfated-β-CD.
A combination of 60 mM α-CD and 0.2 mM sulfated-β-CD was used with a 50 mM acetate buffer, pH 4.03 at 25°C. Three separate peaks were observed on the order of 8 minutes and were resolved efficiently, ($R_{1,2} = 2.96$, $R_{2,3} = 2.43$). It is believed that the nor-LSD and nor-iso-LSD peaks were contained within the observed LSD, LAMPA, and iso-LSD peaks.

Part B: Separation at high pH.

I. Standard peaks using no CD additives.

A. LSD.

A sample of LSD was run with 50 mM borate buffer of pH 8.51 at 25°C. One peak was observed at 4.49 min.

B. LSD and LAMPA.

A sample containing LSD and LAMPA was run with 50 mM borate buffer of pH 8.51 at 25°C. One peak was observed at 4.24 min.

C. LSD and iso-LSD.

Table 6 below summarizes the results using a sample of LSD and iso-LSD with no CD additives.

Trial #	50 mM Borate Buffer pH	Temp (°C)	t_m (min)	R	File	Date; Notebook
1	8.51	25	4.06, 4.27	2.04	BUFTE232-234.D	10/10/02; 019(Y)
2	4.03	25	5.17, 5.26	1.22	BUFTE235-237.D	10/10/02; 019(Y)-020
3	8.51	25	4.05, 4.31	2.48	BUFTE238-240.D	10/10/02; 019(Y)-020
4	9.22	25	5.00, 5.18	1.30	BUFTE241-243.D	10/10/02; 019(Y)-020

C. LSD, LAMPA, and iso-LSD.

Table 7 below summarizes the results using a sample containing LSD, LAMPA, and iso-LSD with no CD additives.

Trial #	50 mM Borate Buffer pH	Temp (°C)	t_m (min)	R	File	Date; Notebook
1	9.22	25	5.04, 5.21	1.54	BUFTE190-192.D	9/23/02; 017(Y)
2	8.51	25	4.48, 4.76	3.83	BUFTE217-219.D	10/8/02; 019
3	8.51	25	4.02, 4.27	3.82	BUFTE244-246.D	10/16/02; 020(Y)
4	8.06	25	3.93, 4.21	5.02	BUFTE253-255.D	10/17/02; 020(Y)-021

II. Separation of samples containing LSD, LAMPA, and iso-LSD.

A. (Aldrich) sulfated-β-CD.

Table 8 below summarizes the results using sulfated-β-CD with an LSD, LAMPA, and iso-LSD sample mixture.

Trial #	[CD] (mM)	50 mM Borate Buffer,pH	Temp (°C)	t_m (min)	R	File	Date; Notebook
1	0.2	9.22	25	5.01, 5.09	0.87	BUFTE193-195.D	9/26/02; 017(Y) - 018
2	0.6	9.22	25	5.40, 5.46	0.38	BUFTE196-198.D	9/26/02; 018
3	10	9.22	25	6.56		BUFTE202-204.D	10/1/02; 018
4	20	9.22	25	7.58		BUFTE205-207.D	10/1/02; 018
5	40	9.22	25	12.51		BUFTE208-210.D	10/7/02; 018(Y)
6	10	8.51	25	6.84, 8.17	18.6	BUFTE220-222.D	10/8/02; 019
7	10	8.51	25	6.38, 7.71	17.9	BUFTE247-249.D	10/16/02; 020(Y)
8	10	8.06	25	No pattern		BUFTE256-258.D	10/17/02; 020(Y)-021

B. Sulfated-α-CD.

Table 9 below summarizes the results using sulfated-α-CD with an LSD, LAMPA, and iso-LSD sample mixture.

Trial #	[CD] (mM)	50 mM Borate Buffer,pH	Temp (°C)	t_m (min)	$R_{1,2}$	$R_{2,3}$	File	Date; Notebook
1	10	9.22	25	6.61, 6.70, 7.02	0.45	2.65	BUFTE211-213.D	10/7/02; 018(Y)
2	20	9.22	25	No peak pattern			BUFTE214-216.D	10/7/02; 018(Y)
3	10	8.51	25	6.32, 6.34, 7.60	0.92	24.2	BUFTE250-252.D	10/17/02; 020(Y)-021
4	10	8.06	25	6.22, 6.32, 7.87	0.96	13.37	BUFTE259-261.D	10/17/02; 020(Y)-021
5	10	8.51	25	6.28, 6.31, 7.72	0.78	27.34	BUFTE262-264.D	10/21/02; 021(Y)
6	15	8.51	25	6.88, 7.05, 8.59	1.53	12.66	BUFTE265-267.D	10/21/01; 021(Y)
7	20	8.51	25	7.54, 7.71, 9.56	1.03	13.45	BUFTE268-270.D	10/21/02; 021(Y)
8	10	8.51	15	7.74, 7.85, 10.09	0.87	14..5	BUFTE271-273.D	10/22/02; 022
9	15	8.51	15	8.83, 9.00, 12.32	1.01	23.9	BUFTE280-282.D	10/22/02; 022
10	20	8.51	15	9.39, 9.73, 13.14	1.52	18.4	BUFTE277-279.D	10/22/02; 022
11*	15	8.51	25	7.03, 7.09, 8.67	1.02	23.8	BUFTE288-290.D	10/25/02; 022(Y)
12*	15	8.51	25	6.94, 6.99, 8.77	0.85	20.4	BUFTE291-293.D	10/25/02; 022(Y)
13*	15	8.51	25	7.09, 7.14, 9.06	0.81	22.0	BUFTE294-296.D	10/28/02; 022(Y)
14*	15	8.51	25	7.28, 7.38, 8.55	0.99	10.8	BUFTE300-302.D	10/29/02; 022(Y)

*Trials used in reproducibility data.

The electropherogram of Trial #11 in Table 9 is included as Figure 16.

Trials #11-14 in Table 9 were performed over a series of five days in order to observe the inter-day reproducibility characteristics of the conditions. The following data describe the averages ± standard deviations, and relative standard deviation values (in parenthesis) for the peak migration times (peak1, peak 2, peak 3) and the resolution ($R_{1,2}$, $R_{2,3}$), respectively; 7.12 ± 0.1 (2%), 7.19 ± 0.2 (2%), 8.78 ± 0.03 (3%), 0.91 ± 0.09 (10%), 18.3 ± 6 (35%). Trials #11-12 were used in the calculations for the following intra-day data; 6.99 ± 0.07 (1%), 7.04 ± 0.08 (1%), 8.72 ± 0.1 (1%), 0.94 ± 0.1 (16%), 22.1 ± 3 (12%).

Figure 16. Separation of LSD, LAMPA and iso-LSD with 15 mM sulfated-β-CD, 50 mM borate buffer, pH 8.51, 25 °C.

Current Electropherogram(s)

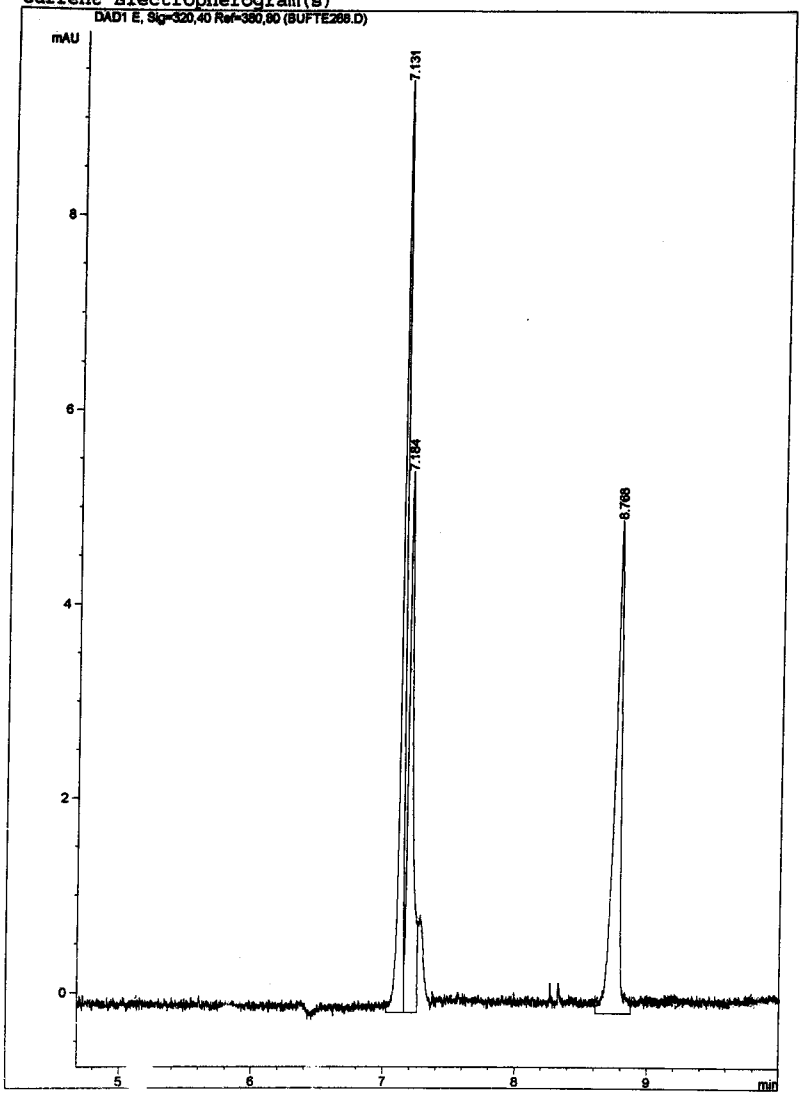

C. Sulfated-α-CD + α-CD.

Trial runs with 20 mM and 40 mM α-CD in combination with 15 mM sulfated-α-CD were analyzed at 15°C. While the second and third peaks produced resolution values well beyond baseline separation ($R_{2,3}$ = 15.8, 26.3), there was little or no separation of peaks 1 and 2 ($R_{1,2}$ = 0.71, 0).

D. (Aldrich) sulfated-β-CD + α-CD.

A combination of 60 mM α-CD and 0.2 mM sulfated-β-CD was used with borate buffer of pH 9.22 at 25°C. The first two peaks were near baseline separation ($R_{1,2}$ = 1.4), but no separation was observed between peaks 2 and 3.

DISCUSSION

Low pH separation of samples containing LSD and LAMPA. In the absence of cyclodextrin additives, separation of the LSD and LAMPA peaks did not occur. The addition of cyclodextrins to the buffer solutions is, therefore, important for analyte separation. The buffer additives introduce the idea of secondary equilibrium. In the following equations, for example, take R to be the cyclodextrin additive, and A and B to be the LSD and LAMPA analytes.[7]

$$A + R \overset{K_A}{\leftrightarrow} AR \quad (6)$$

$$B + R \overset{K_B}{\leftrightarrow} BR \quad (7)$$

In the absence of cyclodextrin, LSD and LAMPA (A and B) have the same charge and mass and, thus, virtually the same electrophoretic mobilities. Under these conditions they are inseparable. Similarly, when cyclodextrins are bound to the LSD and LAMPA (AR and BR), the similar charge and mass of the complexes result in virtually the same electrophoretic mobilities. In other words, the equilibria of Eqs. 6 and 7 cannot be pushed too far to the left, or the right. Therefore, A and B can only be separated when they interact with R differently, or more simply, when K_A does not equal K_B. When K is too small, the equilibria are pushed to the left and, as described in the first scenario, no separation occurs. When K is too large, the second scenario is observed as the equilibria are pushed too far to the right and no separation is achieved. Ultimately, the K value must be intermediate in size, and AR and BR must have a sufficient ΔK for separation to occur. α-CD achieved the best separation of LSD and LAMPA among the various trials using a single cyclodextrin (Table 1). The α-CD produced resolution values on the

order of 2.5 with a difference in peak migration times of about 0.3 minutes (Table 1). Trimethyl-β-CD and dimethyl-β-CD produced no separation, while γ-CD resulted in a resolution of 0.29.

It is believed that the α-CD worked best for the separation of these analytes due to its relatively small hydrophobic cavity, compared to those of β- and γ-CDs. The LSD and LAMPA analytes differ only in the amide portions of the molecules (Figure 1). The smaller α-CD cavity probably has the greatest ability to bind with the analytes at the amide portions only.

A check on the reproducibility of the 60 mM α-CD in 50 mM acetate buffer at 25°C method for the separation of LSD and LAMPA is included in Table 1. With these particular runs, it is observed that inter-day migration times are more variable than those runs performed intra-daily. Resolution values of inter-day trials, however, did not significantly differ. Trial #8, for example, was performed one day earlier, but at approximately the same time during the day as Trial #10. Trial #8 resulted in shorter migration times of 7.58 and 7.95 minutes, than Trial #10 peak times of 7.88 and 8.28 minutes. The resolution values of the two runs, however, are the same (2.49). The percent relative standard deviation (%RSD) values for the inter-day trials were acceptable with values of 2-3% for the migration times, and 3% for the resolution values. Intra-day trends show closer migration time agreement, with similar resolution values. Trials #9 and #11, for example, were performed on the same day. The migration times were similar with 7.92 and 8.32 minutes for Trial #9 and 7.96 and 8.36 minutes for Trial #11. The resolution values were calculated to be 2.48 and 2.51, respectively. The %RSD values for the intra-day trials were less than those for the inter-day runs. Percent relative standard deviation values of 0.5% were calculated for each of the peak migration times, and 0.8% was calculated for the resolution values. Although some variability is observed in both inter-day and intra-day runs, particularly with the migration times, the resolution values are quite reproducible.

Low pH separation of samples containing LSD, LAMPA, and iso-LSD using α-CD. Trial runs with different amounts of α-cyclodextrin were performed in order to determine the optimal concentration for the separation of this three component mixture. The amount of cyclodextrin added determines the extent of CD:analyte complex formation. More cyclodextrin results in more complex formation, and a longer time window for analysis. The 60 mM α-CD run can be compared with the 40 mM and 80 mM runs in Figures 6, 7, and 8, corresponding with Trials #3, 4, and 5 of Table 2, respectively. Resolution values of 0.68 ($R_{1,2}$) and 1.63 ($R_{2,3}$) of the 60 mM α-CD solution determined it as the most optimal CD concentration.

The separation of the three analytes with 60 mM α-CD was improved by lowering the temperature inside the capillary. As the temperature is lowered, the viscosity is increased and the migration times are lengthened. In Trial #4 of Table 2, the temperature was set at 25°C, resulting in migration times of 7.29, 7.38, and 7.64 minutes and resolution values of 0.68 ($R_{1,2}$) and 1.63 ($R_{2,3}$). A temperature of 15°C increased the peak migration times, but improved the resolution of the LSD, LAMPA, and iso-LSD sample mixture. As observed in Trial #15 in Table 2, Figure 9, peak migration times at 15°C were 8.69, 9.34, and 9.48 minutes with resolution values of 1.1 ($R_{1,2}$) and 1.65 ($R_{2,3}$).

A check on the 60 mM α-CD method reproducibility at the lower temperature of 15°C is observed in Trials # 17-19 of Table 2. Both the inter-daily and intra-daily data show a lack of reproducibility. For the intra-day study, the RSD values for the peak migration times are each 5%, while separation of the peaks 2 and 3 was significantly more acceptable ($RSD_{2,3}$ = 4%) than that for the partial separation of peaks 1 and 2 ($RSD_{1,2}$ = 34%). The inter-day reproducibility seems to be much better with RSD values of each of the peaks' migration times below 1%. However, only three of the six injections of the inter-day study were used in the calculations for

the average migration times and resolution values. The other three injections resulted in only two peaks and could not be used in the averages. Even the partial separation of the three included injections was not very reproducible with RSD values of 66% and 18% for peaks 1 and 2, and peaks 2 and 3, respectively.

Low pH separation of samples containing LSD, LAMPA, and iso-LSD using α-CD and sulfated-β-CD. Although the use of 60 mM α-CD achieved adequate separation of the three analytes, an even better separation resulted when a charged CD was introduced to the system. Since the analytes form host:guest complexes with the cyclodextrin additives, the charge on the sulfated-β-CD complexes is also of importance. The effect is demonstrated in the addition of 0.2 mM sulfated-β-CD to 60 mM α-CD in a 50 mM acetate buffer solution (Trial # 14 of Table 3; Figure 10). Even though the sulfated cyclodextrin was present in such a small amount, a second dynamic system was introduced within the capillary. The analytes could partition between both the α-CD and the sulfated-β-CD. Although the separation required a longer time window to complete (~14 minutes), the added charge on the CD made it possible to separate the analyte peaks with extremely good resolution ($R_{1,2} = 3.15$, $R_{2,3} = 2.7$).

The reproducibility of this method was investigated over the course of several days. Trials # 9-11 in Table 4 include the migration times collected and the calculated resolution values. The shorter migration times relative to the earlier trials is most likely due to the several washings of the column that occurred prior to these particular trials. The reproducibility is more acceptable for the intra-day runs than for those performed inter-daily. While the average migration times for Trials #9 and 11 are quite close, those of Trial #10 are more than half a minute later and create high RSD values (RSD = 4-5%). The resolution values of these runs

grew progressively better, and high RSD values were calculated ($R_{1,2} = R_{2,3} = 14\%$). Intra-day data, however, were relatively better. The data are based on six successive injections included in Trial #11. The peak migration times each had an RSD value of 1%, while the RSD values for peaks 1 and 2, and peaks 2 and 3, were 2% and 5%, respectively.

The buffer concentration is another important experimental variable in CE. The concentration of buffer has an effect on the electroosmotic flow, which affects the migration times. The electroosmotic flow (Eq. 3) depends on the zeta potential, ζ, which is the potential at the liquid-solid interface. The zeta potential is directly proportional to the number of capillary wall charges and inversely proportional to the buffer concentration. As the concentration of buffer is increased, there are more cations in solution. The excess cations shield the analytes from charge and the zeta potential is lowered. Also, the frictional drag on the ions moving toward the detector is increased, which reduces the electroosmotic flow. The sample mixture, therefore, moves more slowly through the capillary, thereby increasing the migration times. In order to optimize the buffer concentration, 25 mM, 50 mM, and 75 mM acetate buffer solutions were used in Trials # 3, 4, and 5 of Table 3. The resulting electropherograms are included in Figures 11, 12 and 13. As buffer concentration increased, peak migration times increased as a result of decreased EOF. The resolution of the peaks decreased. With the 75 mM acetate buffer, for example, no separation of the three analytes was achieved (Figure 13). The best combination of short migration times (10.12, 11.24, and 11.76 minutes) and high resolution ($R_{1,2} = 6.93$, $R_{2,3} = 2.23$) was observed with the 25 mM acetate buffer (Figure 11). However, it was difficult to reproduce these results in successive runs. Thus, the 50 mM acetate solution was determined as the optimal buffer for the separation of LSD, LAMPA, and iso-LSD (Figure 12). At this

concentration, the peaks were observed at 10.83, 12.30, and 12.61 minutes, and had resolution values of 11.4 ($R_{1,2}$) and 1.73 ($R_{2,3}$) in the separation of the three analytes.

Low pH separation of samples containing LSD, LAMPA, and iso-LSD using sulfated-β-CD. The pH of the buffer solution is important to maximize the magnitude and reproducibility of the electroosmotic flow of a CE run. At higher pH values (> pH 8), the electroosmotic flow is greatest due to the maximum ionization of the silica groups at the capillary wall. The increase in ion velocity shortens the migration times and also sharpens the peak shape, which generally results in a more reproducible CE run. A solution of 50 mM acetate buffer at a pH of 4.03 and containing 0.3 mM sulfated-β-CD, was tried first in the separation of LSD, LAMPA, and iso-LSD (Trial #3 of Table 5, Figure 14). At this particular pH, the combination of acetate buffer and CD baseline-separated the three analytes in about a thirteen minute time window (11.68, 13.3, and 13.7 minutes). The reproducibility (RSD 2-3%) with the buffer, however, is a problem since the EOF is highly dependent on pH in the pH 4-6 range.[8] Instead, it is at higher pH values that better reproducibility should be obtained because of a more constant electroosmotic flow. A solution of 0.3 mM sulfated-β-CD in a 50 mM borate buffer of pH 8.51 was then used with the LSD, LAMPA, and iso-LSD sample. The buffer and CD combination, however, was unable to completely separate the three analytes (Trial #6 of Table 5, Figure 15). Only two peaks are observed at pH 8.51; they are sharp and have migration times on the order of five minutes (4.71 and 4.84 minutes).

Low pH separation of samples containing LSD, LAMPA, and iso-LSD using α-CD polymer. While α-CD is considered to be most ideal due to its relatively small hydrophobic cavity, the characteristic was not observed for the α-CD polymer. The α-CD polymer is composed of α-CD units linked together with glyceryl units. No analyte peaks were observed with 60 mM α-CD polymer. Furthermore, when the concentration of the polymer was decreased to as low as 10 and 20 mM, just two peaks were resolved.

High pH separations in the absence of cyclodextrin. No separation was observed between LSD and LAMPA at high pH without the addition of cyclodextrin. Upon trials with LSD and iso-LSD, however, some separation was achieved. The results of several trials at different pH values are included in Table 6. At pH 8.51, in Trials #1 and 3, LSD and iso-LSD are observed as two baseline-separated peaks (R~2.2) at about 4.05 and 4.30 minutes. LSD and iso-LSD remain separated upon the addition of LAMPA, as well. Table 7 summarizes the results obtained with trials of samples containing LSD, LAMPA, and iso-LSD. Although LSD and LAMPA are observed as one peak, LSD and iso-LSD are separated with even better resolution than in previous trials with the two analytes only. In Trial #3 of Table 7, for example, the migration times of the peaks are very similar with 4.02 and 4.27 minutes, while the resolution increased to 3.82. It is believed that LSD and iso-LSD are separated without the use of cyclodextrins due to a slight pKa difference at the ring nitrogen atom, which results from the different orientations of the amide portions of the molecule. LSD and LAMPA, however, lack the difference in orientation and the pKa values are nearly identical.

High pH separation of samples containing LSD, LAMPA, and iso-LSD using sulfated-α-CD. LSD and LAMPA have the same mass and virtually the same charge. At a pH of 8.51, buffers containing charged cyclodextrins could separate a sample mixture containing LSD, LAMPA, and iso-LSD by changing both the effective charge and mass of the analytes. While both sulfated-α- and sulfated-β-CDs were tried in the separation of the three component mixture, only sulfated-α-CD trials resulted in three resolved peaks. Concentrations of 10, 15, and 20 mM sulfated-α-CD were tried with 50 mM borate buffer of pH 9.22, 8.51, and 8.06. The most ideal separation resulted from 15 mM sulfated-α-CD in borate buffer of pH 8.51 (Table 9, Trial #11; Figure 16). The higher CD concentration of 20 mM resulted in baseline shifts and background noise at lower wavelengths due to the absorption characteristics of the sulfate group. The lower CD concentrations (10 mM) did not resolve the two LSD and LAMPA peaks with as well as did 15 mM sulfated-α-CD.

A reproducibility check on the 15 mM sulfated-α-CD with 50 mM borate buffer of pH 8.51 at 25°C was performed and the results are included in Table 9. Inter-day calculations were performed with the results of Trials #11-14. While peaks 1 and 2 (7.12 ± 0.1 and 7.19 ± 0.2 minutes, respectively) were fairly reproducible with an acceptable RSD value of 2% and with resolution of 0.91 ± 0.09, RSD = 10%, more deviation was observed in the third iso-LSD peak. With an average migration time of 8.78 ± 0.3 minutes and RSD of 3%, there is more variability in the resolution value ($R_{2,3}$ = 18.3 ± 6, RSD = 35%). The significant degree of separation between peaks 2 and 3, however, tends to overshadow the lack of reproducibility.

Similar intra-day calculations were performed for the 15 mM sulfated-α-CD at pH 8.51 separation method using the six injections of Trials #11 and 12. In the intra-daily runs, the reproducibility of the third peak was more acceptable than in the inter-daily runs. Furthermore,

the migration times of each of the three peaks, 6.99 ± 0.07, 7.04 ± 0.08, and 8.72 ± 0.1 minutes, respectively, were each acceptable with RSD values of 1%. The resolution values between the first two peaks ($R_{1,2}$) were on the same order of magnitude with an average of 0.94 ± 0.1 and an RSD of 16%. Due to the reproducibility of the third iso-LSD peak, however, the intra-day $R_{2,3}$ value is significantly better than that of the inter-day trials ($R_{2,3}$ = 22.1 ± 3, RSD = 12%).

CONCLUSIONS

Three methods in particular stand out for the separation of LSD and the other similarly structured molecules.

The 60 mM α-CD in a 50 mM acetate buffer, pH 4.03 at 15°C (Trial #15, Table 2; Figure 9) resulted in three analyte peaks in the following order; LSD, iso-LSD, LAMPA. While peaks 2 and 3 were baseline separated (R = 1.65), peaks 1 and 2 displayed some overlap with a resolution value of 1.1. Also, while the resolution was reproducible, the migration times were less so from inter-day, as well as intra-day analyses. The low pH certainly contributes to the problem, but the intra-day variation may be evidence of build-up on the capillary walls. The problem may be avoided at a higher pH, which allows greater, more reproducible electroosmotic flow and shorter migration times.

The combination of 60 mM α-CD and 0.2 mM sulfated-β-CD in the same 50mM acetate buffer, pH 4.03 at 25°C (Trial #14, Table 3; Figure 10) is the most reproducible method at low pH. Here, the order of analytes was observed with iso-LSD first, followed by LSD and LAMPA, respectively. This method resulted in resolution values as high as 5.4 and reproducible intra-day RSD values of 1% for the peak migration times, and 2% and 5% for $R_{1,2}$ and $R_{2,3}$, respectively. While the inter-day data was not as reproducible, the method may still be used qualitatively for the separation of LSD, LAMPA, and iso-LSD.

The other comparable separation method occurred at a higher pH value of 8.51 (Trial #11 Table 9; Figure 16). The separation with 15 mM sulfated-α-CD in 50 mM borate buffer at 25 °C resulted in LSD and LAMPA peaks first, followed by one for iso-LSD. Once again, intra-day reproducibility of migration times was better than inter-day data. RSD values for inter-day runs ranged from 2-3%, while intra-day data was just 1%. The partial separation (R = 0.9) of peaks 1

and 2 remained about the same, but $R_{2,3}$ data was much different. In all cases, peaks 2 and 3 were separated with resolution values above 10.0, which are well beyond the acceptable baseline separation value of 1.5.

REFERENCES

1. New York State Police Crime Laboratories, Drug Chemistry Technical Manual. 5/10/02 - 12/31/02; pp 50-52.

2. Harris, Daniel C. *Quantitative Chemical Analysis. Fifth Edition.* W.H. Freeman and Company: New York, 1998; pp 772.

3. Weinberger, Robert. *Practical Capillary Electrophoresis. Second Edition.* Academic Press: San Diego, 2000; pp 32.

4. Weinberger, Robert. *Practical Capillary Electrophoresis. Second Edition.* Academic Press: San Diego, 2000; pp 40.

5. http//www.natur.cuni.cz/~jindrich/CD/. Jindrich Jindrich, Department of Chemistry; Charles University; Prague, Czech Republic.

6. Werner, T.C., Colwell, K., Agbaria, R.A., Warner, I.M. Applied Spectroscopy. 1996, 50, 512.

7. Weinberger, Robert. *Practical Capillary Electrophoresis. Second Edition.* Academic Press: San Diego, 2000; pp 95.

8. Weinberger, Robert. *Practical Capillary Electrophoresis. Second Edition.* Academic Press: San Diego, 2000; pp 35.